2012

MUTANT P53 REGULATION OF CXC-CHEMOKINE EXPRESSION IN HEAD AND NECK SQUAMOUS CELL CARCINOMA

Brittany Field
Virginia Commonwealth University

MUTANT P53 REGULATION OF CXC-CHEMOKINE EXPRESSION IN HEAD AND NECK SQUAMOUS CELL CARCINOMA

A Thesis submitted in partial fulfillment of the requirements for the degree of Master of Science at Virginia Commonwealth University.

by

BRITTANY LEIGH FIELD
Bachelor of Arts in Biology, University of Virginia, 2008

Director: DR. W. ANDREW YEUDALL
PHILIPS INSTITUTE, VCU SCHOOL OF DENTISTRY

Virginia Commonwealth University
Richmond, Virginia
December, 2012

Acknowledgement

I first would like to thank my P.I., Dr. Andrew Yeudall, for giving me the opportunity to do research in his laboratory and most importantly, for taking the time and effort to teach me the skills I needed to successfully complete my thesis. I greatly appreciate his patience with my constant questions and need to check and double-check before doing new experiments, especially with calculations. I also thank Dr. Hiro Miyazaki for the thought-provoking feedback given during lab meeting presentations that provided a fresh perspective on my results to help in my defense preparation. I also would like to thank my lab-mates who were always available to answer questions, give advice, or simply listen to the frustrations of an experiment gone wrong: Anna Bulysheva, Chris Holden, Shreya Desai, Rubana Masood, Young Kim, and Robert Swenson. Additionally, I thank Shreya Desai in particular for putting up with me throughout the past year of classes, research, and T.A.-ing. I look forward to working with her for the next five years in dental school. Next, I would like to thank the members of my advisory committee, Dr. Sumitra Deb, Dr. Liya Qiao, and Dr. John Grider, for their time and commitment. Last, but certainly not least, I would like to thank my family and friends for always believing in me.

Table of Contents

Page

List of Tables

Page

List of Figures

Page

Abbreviations

CXCL	C-X-C motif chemokine ligand
CXCR	C-X-C motif chemokine receptor
DBD	DNA-binding domain
ΔN	Amino-deleted
EGF	Epidermal growth factor
EGFR	Epidermal growth factor receptor
EPS8	Epidermal growth factor receptor kinase substrate 8
GOF	Gain-of-function
GPCR	G-protein coupled receptor
HNSCC	Head and neck squamous cell carcinoma
HPV	Human papillomavirus
miRNA	microRNA
MMP	Matrix metalloprotease
OD	Oligomerization domain
SAM	Sterile alpha motif
siRNA	Small interfering RNA
TA	Transactivation domain
TGF-α	Transforming growth factor alpha
TID	Transactivation inhibitory domain
VEGF-C	Vascular endothelial growth factor - C

Abstract

MUTANT P53 REGULATION OF CXC-CHEMOKINE EXPRESSION IN HEAD AND NECK SQUAMOUS CELL CARCINOMA

By Brittany Leigh Field, MS

A Thesis submitted in partial fulfillment of the requirements for the degree of Master of Science at Virginia Commonwealth University.

Virginia Commonwealth University, 2012.

Major Director: Dr. W. Andrew Yeudall
Philips Institute, VCU School of Dentistry

Head and neck squamous cell carcinoma (HNSCC) is the 6th most common type of cancer in the western hemisphere with a five-year survival rate of only 50% for patients with a localized tumor, which decreases significantly to as low as 5% for those patients with tumors that have metastasized to distant sites of the body. It has been found that both mutant p53 and epidermal growth factor receptor (EGFR) signaling pathways function to increase the expression of CXCL5, which has been identified as a key mediator in the process of tumor metastasis. Previous data from our lab suggested that the p53 homolog, p63, may function as a negative regulator of CXCL5 and that mutant p53 may inhibit this molecule to elevate CXCL5 expression levels.

In the current study we utilized an model system in which the H179L p53 mutant was expressed in HN4 cells to investigate the hypothesis that mutant p53 enhances expression of CXCL5 by both interfering with p63 function and cooperating with EGFR/EPS8 signaling, leading to increased cell proliferation and motility. The results of the current study indicate a role for mutant p53 in head and neck squamous cell carcinoma proliferation, migration and tumorigenicity, possibly through enhancement of CXCL5 expression. We were able to show that mutant p53 expression caused an increase in the expression of this chemokine in addition to increasing proliferation and migration of the cells compared to the vector control. Additionally, we showed that p63 protein is a negative regulator of CXCL5 that is downregulated in the cells expressing mutant p53, which suggests that through direct interaction, mutant p53 may function to inhibit p63 function as well as target it for degradation. These results support the hypothesis that GOF mutant p53 enhances expression of CXCL5 by interfering with p63 function in cancer cells. The results of the current study results also showed that upon treatment with EGF, HN4 cells expressing mutant p53 express elevated levels of CXCL5; and that the mutant p53-expressing HN4 cells cooperate with EGFR/EPS8 signaling to further deregulate chemokine expression. These data taken together suggest there are complex interactions taking place between mutant p53, p63, EGFR signaling, and CXCL5 to regulate the biological processes that promote tumor progression that could lead to metastasis. Additional studies are needed to further elucidate the molecules involved in the mutant p53 mechanism that promotes tumorigenesis.

Introduction and Background

1.1 Head and Neck Squamous Cell Carcinoma (HNSCC)

Head and neck squamous cell carcinoma (HNSCC) is the name given to cancers that begin in the mucosal lining epithelial cells of the upper aerodigestive tract (1), which includes cells of the oral cavity, tongue, pharynx, larynx, and paranasal sinuses (2). HNSCC is the 6th most common type of cancer in the western hemisphere with a five-year survival rate of 50% for patients with a localized tumor (2). Death typically occurs as a result of uncontrolled disease progression, both because of recurring local primary tumor and because of metastasis to distant sites in the body (1). Metastasis is the major reason for poor survival rates that drop as low as 5% despite continued efforts to improve treatments (3).

Two risk factors that have been identified as causes of head and neck squamous cell carcinoma are tobacco and alcohol use (4, 5) with tobacco use being the main contributor. The carcinogens present in tobacco smoke have genotoxic effects on the head and neck epithelial cells, which can lead to mutations that can result in tumor formation. In particular, there is a link between tobacco use and mutations in the p53 tumor suppressor gene (6), which can lead to spontaneous tumor formation (7). Alcohol primarily functions to synergistically amplify the effects of tobacco use, but its metabolite, acetaldehyde, can

also form DNA adducts that can impede DNA repair (8). An additional risk factor in HNSCC is human papillomavirus (HPV), which targets basal mucosal epithelial cells and transforms them into either a benign form, or high-risk type that can progress to a cancerous lesion (4).

1.2 Tumor Metastasis

Head and neck squamous cell carcinoma is a result of a multi-stage process that begins with an accumulation of mutations in normal epithelial cells (9, 10). Mutations result in the silencing of tumor suppressors and overexpression (or altered forms) of oncogenes (9), allowing for alterations to the normal processes that regulate growth and migration, as well as cell differentiation and death (2).

Accumulation of genetic damage (10) causes normal epithelial cells to progress through multiple stages of premalignant lesions and can eventually form a malignancy (11). The cells of the primary tumor secrete factors such as VEGF-C that promote their growth (12) and cross-talk with the mesenchyme-derived stromal fibroblasts, to further increase cell proliferation (2). This interaction between the mesenchyme and the epithelial cells results in paracrine activation, which plays a key role in tumorigenesis (13). Secreted factors also favor angiogenesis by migration of endothelial cells, and in addition, these factors promote the migration of immune cells. The chemokines CXCL5 and CXCL8 have been identified as key mediators of this inflammatory component of tumor progression (14). As the tumor develops, cells can degrade the extracellular matrix by secreting matrix metalloproteases, such as MMP-9 (15) and migrate toward a chemokine gradient (16). This

process of metastasis involves the interaction of these primary tumor cells with normal epithelial cells, the extracellular matrix, and other associated factors (3). HNSCC metastasis usually occurs by tumor cells entering lymph vessels, to be carried to loco-regional or distant sites in the body (2, 17). The target organs express ligands for receptors expressed on the surface of tumor cells, resulting in a "homing mechanism" that favors migration (18). The tumor cells that metastasize and colonize a secondary site at a lymph node must develop survival mechanisms allowing for the development of a secondary lesion (2).

1.3 Chemokines

Chemokines are a family of small, secreted chemoattractant proteins that are classified based on the relationship between conserved cysteine residues (19). The four subfamily groups are named CXC, CC, XC, and CX_3C, shown in Figure 1. CXC-chemokines contain two cysteines separated by one residue, CC-chemokines have two adjacent cysteine residues, XC-chemokines only have one disulfide bond, and CX_3C-chemokines contain two cysteines separated by three residues. What is unique about CX_3C-chemokines is that they contain a mucin-like stalk at the C-terminus, which allows this molecule to embed into cell membranes, but there is only one known member of this subfamily (19). All chemokines have a conserved 'Greek key' supersecondary structure (shown in Figure 1), which is composed of three connected antiparallel β-strands plus an α-helix that is positioned next to the first β-strand, but connected to the third (19). CXC-chemokines can be further divided based on whether they contain the glutamic acid-

leucine-arginine (E-L-R) amino acid motif N-terminal to the cysteines. ELR+ CXC-chemokines, such as CXCL5, typically function as chemoattractants (2) and have been linked to the process of tumor formation (14).

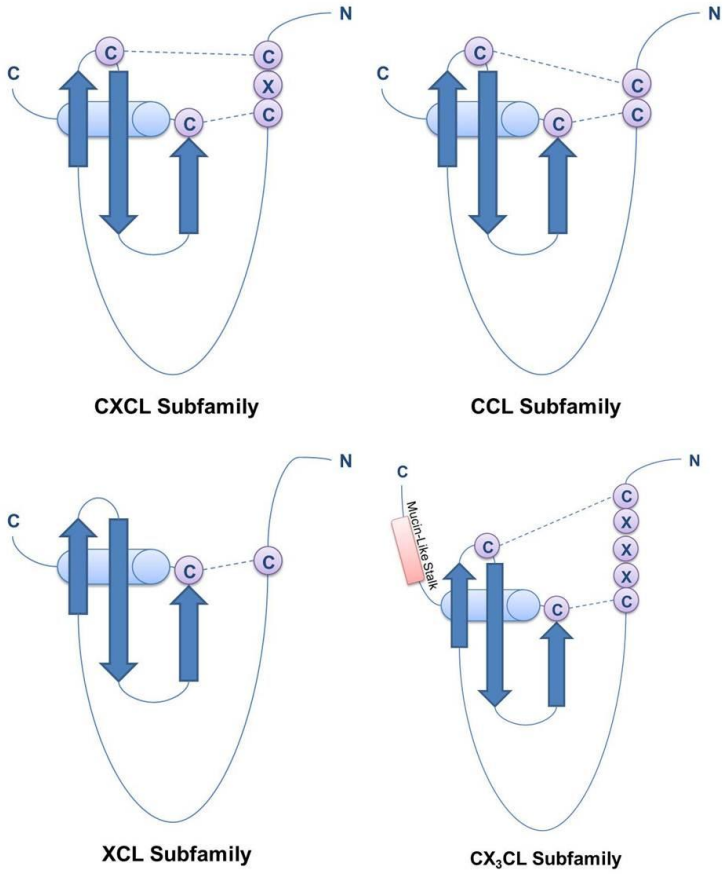

Figure 1. Chemokine classification by the spacing of conserved cysteines. Figure modified according to (19).

1.4 Chemokine Receptors

Chemokine receptors are members of the G-protein coupled receptor (GPCR) class A rhodopsin-like family and are composed of an extracellular domain that includes the N-

terminus plus 3 loops that work together to bind the chemokine ligand. The intracellular domain includes the C-terminus and also contains three loops that transduce the chemokine signal (16). Chemokines either bind to a specific GPCR family receptor or activate more than one in a promiscuous manner (2). A receptor can also be activated by more than one chemokine ligand, as shown in Figure 2. Typically, CXC-chemokines activate CXCR receptors and CC-chemokines only activate CCRs (19).

	Receptor	Ligand
CXC-	CXCR1	CXCL6, CXCL8
	CXCR2	CXCL1, CXCL2, CXCL3, CXCL5, CXCL6, CXCL8
	CXCR3	CXCL4, CXCL9, CXCL10, CXCL11
	CXCR4	CXCL12
	CXCR5	CXCL13
	CXCR6	CXCL16
	CXCR7	CXCL11, CXCL12
CC-	CCR1	CCL3, CCL5, CCL7, CCL8, CCL13, CCL14, CCL15, CCL16, CCL23
	CCR2	CCL2, CCL7, CCL8, CCL13, CCL16
	CCR3	CCL5, CCL7, CCL8, CCL11, CCL13, CCL15, CCL24, CCL26, CCL28
	CCR4	CCL17, CCL22
	CCR5	CCL3, CCL4, CCL5, CCL8, CCL16
	CCR6	CCL20
	CCR7	CCL19, CCL21
	CCR8	CCL1
	CCR9	CCL25
	CCR10	CCL27, CCL28
CX_3C-	CX_3CR1	CX_3CL1
C-	XCR1	XCL1, XCL2

Figure 2. Both specific and promiscuous relationships exist between chemokine family ligands and receptors. Figure modified according to (2).

1.5 CXCL5 Role in HNSCC

Chemokines normally function in a chemotactic manner to promote the movement of pro-inflammatory cells to the site of inflammation by creating a chemokine gradient. Chemokines are related to both this normal inflammatory response (17) and to the inflammatory component of cancer metastasis in which the chemokine system is "hijacked" by tumor cells. Chemokines favor tumor progression by increasing tumor cell proliferation and migration (14). Chemokines are also involved with promoting angiogenesis (12).

A specific chemokine of interest is CXCL5, which binds to and activates the receptor CXCR2 (2). The expression of chemokines and their receptors is normally a tightly-regulated process governed by cytokines and growth factors, but CXCL5 has been shown to have increased expression in metastatic cells compared to primary tumor cells. This suggests the regulation is altered during tumor progression (18). Previous studies have shown that inhibiting the expression of this chemokine can reduce tumor cell migration and invasion as well as block tumor formation *in vivo* (18), which suggests the interaction between CXCL5 and CXCR2 is an important mediator in the formation of metastasized tumors. Blocking CXCR2 has been identified as a potential therapeutic target to inhibit tumorigenesis (2).

1.6 p53

p53 is a transcription factor and normally functions as a tumor suppressor by inducing cell cycle arrest and DNA repair or apoptosis in response to genotoxic cell stress.

In this way, p53 prevents proliferation, protects the genome, and eliminates damaged cells (7). In over half of all human cancers, however, p53 is mutated or inactivated (7), an event that is crucial for the initiation of cancer formation (20). Most of these amino acid substitution mutations are found in the DNA-binding domain (Figure 3A) and result in an aberrant protein with new gain-of-function oncogenic properties (21).

Previous studies with lung cancer cells have shown that one of these new functions of mutant p53 involves the upregulation of CXCL5 expression as measured by the activity of the CXCL5 promoter and transcript levels (20). Wild-type p53 actually functions to repress CXCL5 (20) so a loss of wild-type p53 function is sufficient to induce CXCL5 expression, while mutant p53 upregulates CXCL5 further (20).

1.7 H179L Mutant p53

The H179L p53 protein carries a histidine-to-leucine amino acid substitution at codon 179, which is located in the DNA-binding domain (21). Previous studies have shown that expression of the H179L p53 mutant can transform immortal cells into a metastatic phenotype. This shows that a single missense mutation results in a p53 mutant that has lost its wild-type function (22) and can act in a dominant negative manner to inhibit wild type p53 and possibly other family members (21, 23).

There are several possible mechanisms by which mutant p53 might enhance CXCL5 expression, shown in Figure 3. These include mutant p53 inhibition of its family member, p63 (24), direct binding of mutant p53 to the CXCL5 promoter region to activate gene expression (20), or activation of NF-κB2 (20) or other transcription factors we have

yet to identify. Thus far, GOF mutant p53 has not been demonstrated to bind to the CXCL5 promoter. This raises the possibility that additional steps, carried out by other proteins, are necessary for regulation of CXCL5.

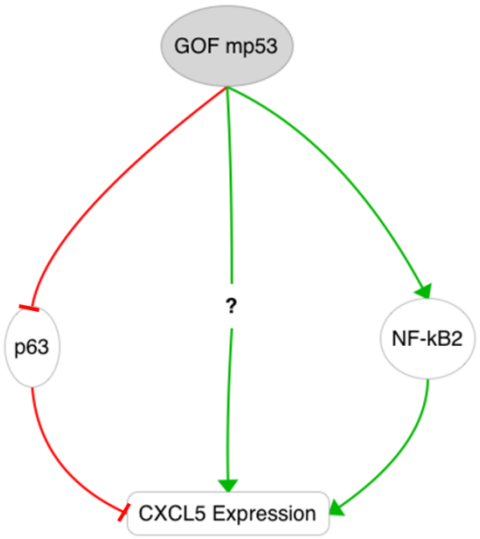

Figure 3. Three of the possible mechanisms by which mutant p53 might activate CXCL5 expression.

1.8 p63

p53 is one member of a family of transcription factors that includes p73 and p63 (25, 26), the latter of which is highly relevant for the development of stratified epithelial tissues, such as the epidermis that functions as a barrier and waterproof seal for the body (7). p63 knock-out mice have developmental defects, specifically a lack of any stratified squamous epithelium and associated structures such as complex glands. These mice also have limb truncations and craniofacial abnormalities, but because of the lack of an

epidermis, they do not survive. Together, these observations suggest a crucial functional role for p63 in development (7), but p63 also has a distinct role in adulthood, particularly in cancer (7). These two different roles played by one molecule are another component adding to the controversy surrounding the function of p63 (24).

Another layer of this controversy is the fact that there are six different p63 isoforms, arising from two separate promoters plus alternative splicing at the C-terminus, shown in Figure 4. All of the isoforms share a common core domain composed of the DNA-binding domain (DBD) and oligomerization domain (OD), which have 60% and 37% homology to the corresponding domains of p53. TA-isoforms arise from the first promoter and contain the transactivation domain (TA) that the ΔN-isoforms lack because they begin at the second promoter. Additional alternative splicing of the p63 mRNA at the C-terminus yields α-, β-, and γ-isoforms. p63α-isoforms contain a sterile alpha motif (SAM) that is important in protein-protein interactions and a transactivation inhibitory domain (TID) that the shorter p63β- and p63γ-isoforms lack (7, 27).

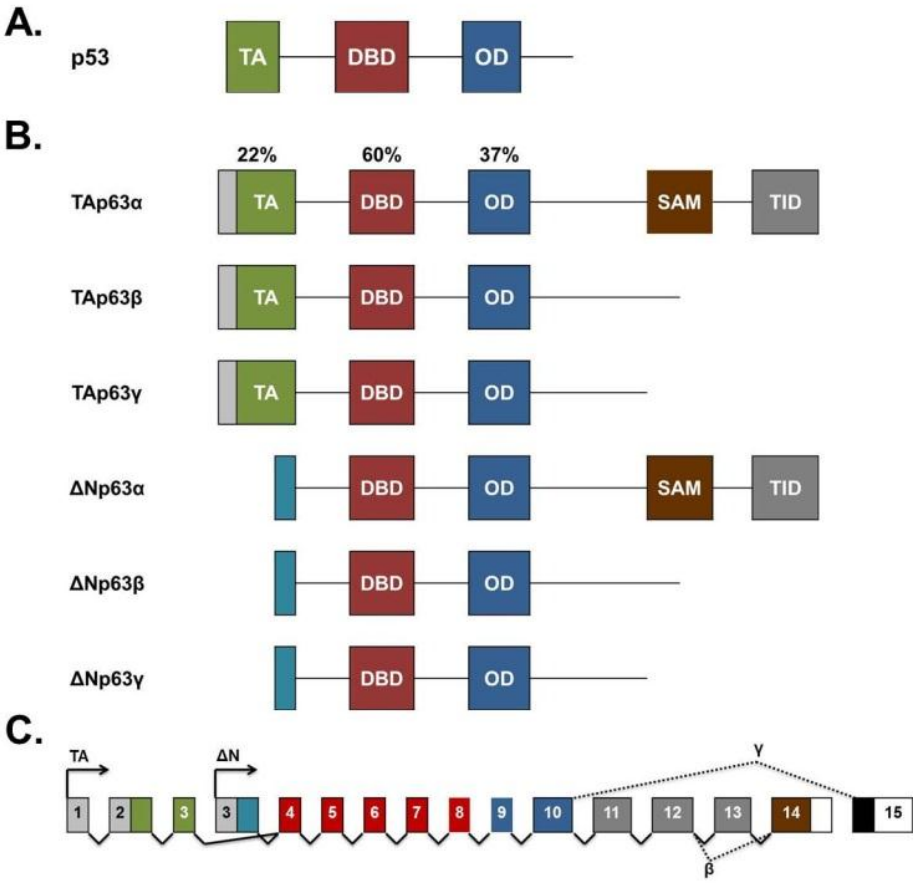

Figure 4. Two promoters plus alternative splicing form six p63 isoforms. (A) Functional domains of p53 tumor suppressor. (B) Functional domains of p53 homolog, p63. Percentages show identical residues between p53 and p63. (C) Two separate promoters and alternative splicing patterns of the p63 mRNA transcript to create six individual isoforms. Figure modified according to (7).

The six different p63 isoforms that have distinct structures also have a variety of functions, which adds to the complexity of the p63 controversy (24). ΔN-isoforms lack the N-terminal transactivation domain and act as dominant inhibitors (28) of TAp63 and wild type p53 tumor suppressive function (7, 27). These oncogenic isoforms (22) have been shown to inhibit terminal differentiation and promote early tumorigenesis. In both normal

epithelial cells and in HNSCC cells, ΔNp63α is the major isoform at the protein level (28). ΔNp63 isoforms have also been shown to upregulate the expression of the stem cell marker and cell surface glycoprotein, CD44, which is involved in cell migration and adhesion. Additionally, p63 activates keratins required for proliferation, while it downregulates other keratins to cause a more invasive cell phenotype (29). TA-isoforms are primarily located in differentiated cells higher in the epithelium, while ΔN-isoforms are localized to the basal epithelial cells and are considered epithelial stem cell markers (24, 29). ΔNp63α has been identified in stem cells of the breast and prostate (27). ΔN-isoforms are expressed at the barrier between epithelium and mesenchyme, and a loss of p63 has been associated with epithelial mesenchymal transition (EMT) in which epithelial cells acquire traits more common to mesenchymal cells (3). The mesenchymal phenotype is associated with increased metastatic potential (25). Although the different isoforms have been linked to certain functions, it isn't completely clear yet which isoform causes each phenotype. Additionally, different cell types express different levels of the p63 isoforms (27). Changes in isoform expression are thought to play a role in tumorigenesis by affecting cell proliferation and differentiation (27). The large number of targets regulated by p63 (29), including transcription factors, adhesion and signaling molecules, and regulatory microRNAs (miRNAs) (30), further complicates our understanding of p63 function.

Unpublished data from our lab show that inhibiting p63 in lung cancer cells results in enhanced CXCL5 expression and increased cell motility (W.A. Yeudall, unpublished data), which suggests that p63 might act to repress CXCL5 expression. This change in CXC-chemokine expression in response to decreased p63 is not observed in normal

epithelial cells, suggesting this may be an acquired characteristic of tumor cells (34). Additional studies have shown that a loss of p63 results in an increase in the expression of genes that favor invasion and metastasis (25, 32), as measured by microarray analysis, and that p63 inhibition also causes an increase in squamous carcinoma cell migration (25). A loss of p63 has been associated with poor prognosis in some cancers (25). It has also been shown that, by interacting with p63, mutant p53 can repress the normal p63 function to inhibit metastasis in lung cancer cells (24), which is another reason why we are investigating a similar mechanism in an oral cancer cell model.

1.9 Epidermal Growth Factor Receptor (EGFR) Signaling

Another important aspect of epithelial tumor progression is the epidermal growth factor receptor (EGFR) signaling pathway (33). The EGFR is a member of the ErbB family of receptor tyrosine kinase and is activated by the binding of EGF-family ligands such as EGF and TGF-α (33). Ligands can bind either of two extracellular ligand-binding sites (L1 and L2 in Figure 4), which induces receptor dimerization with another EGFR via the cysteine-rich domains (S1 and S2 in Figure 4). This results in transphosphorylation of cytoplasmic tyrosine residues by the intrinsic protein tyrosine kinase activity, which promotes docking of SH2-containing proteins to the cytoplasmic domain of the EGFR (33). Finally, downstream targets are activated to initiate a biological response (13, 15).

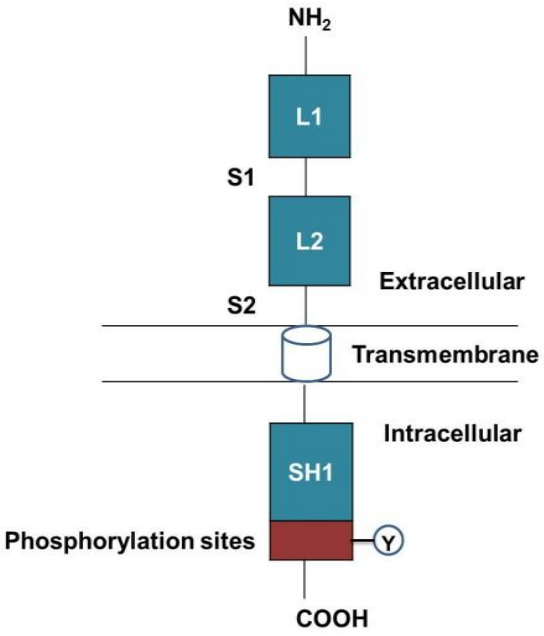

Figure 5. Structure of the EGFR monomer. L1 and L2: ligand-binding sites; S1 and S2: cysteine-rich domains; SH1: protein tyrosine kinase domain. Figure modified according to (13).

This signaling pathway normally functions in differentiation and development, migration, apoptosis, and wound healing (13). EGFR signaling enhances motility through signal transduction to the actin cytoskeleton, and invasion by promoting the expression of matrix metalloproteases that degrade the extracellular matrix (3). Previous studies from our lab using microarray analysis have shown that treatment of cells with EGF causes an increase in the expression of many genes favoring metastasis, including CXCL5 (18). EGF receptors and ligands are often overexpressed in human cancers, allowing for autocrine or paracrine cell stimulation, leading to altered gene expression (15). Overexpression of EGFR in HNSCC makes it a potential therapeutic target (28).

EGFR signaling has also been linked to p63. One study showed that treatment of human epithelial cells with EGF resulted in decreased expression of p63 (34), while another study with pancreatic ductal adenocarcinoma cells showed that treatment with EGF caused an increase in ΔNp63α-induced motility. This same study showed that overexpression of ΔNp63α also resulted in EGFR upregulation (10). A third study showed decreased p63 expression in HNSCC cells upon treatment with an EGFR inhibitor (28) and it has been suggested that in HNSCC, EGF regulates ΔNp63α through the downstream mediator, PI3K (7).

1.10 EPS8 Role in HNSCC

EPS8 is a downstream mediator of the EGFR signaling pathway shown to have increased expression in metastasized tumor cells (15). Previous data indicate that EPS8 upregulates the expression of the FOXM1 transcription factor, resulting in increased CXCL5 expression along with increased cell growth and motility (35). It has also been shown that inhibition of FOXM1 causes a reduction in CXCL5 expression (35). FOXM1 has not been localized to the CXCL5 promoter, which raises the possibility that the increase in chemokine expression is mediated by other molecules. EPS8 has also been shown to be involved with the EGFR-induced upregulation of MMP-9, which is important for matrix degradation and processing of both growth factor and cytokine ligands (15). Both processes contribute to tumor metastasis and are shown in Figure 6.

The observed increase in CXCL5 expression seen with activation of the EGFR/EPS8 signaling pathway provides rationale for looking at the cooperativity between

the mutant p53 and EGFR/EPS8 regulation of CXCL5 expression. Our goal is to determine whether these pathways independently enhance the expression of this chemokine or if they act through the same pathway.

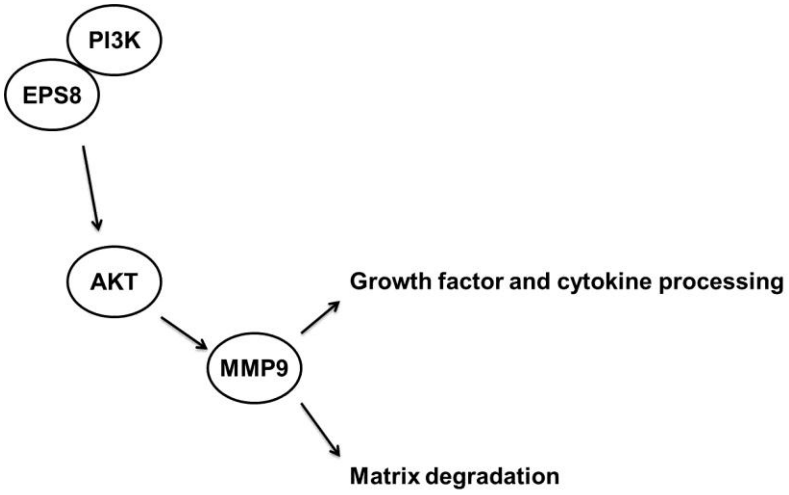

Figure 6. EPS8 activates expression of matrix metalloproteases. Figure modified according to (15).

1.11 Model System

For our model system, we chose primary tongue tumor HN4 cells and metastasized lymph node HN12 cells, derived from the same patient. These cells were chosen because HN4 cells express high levels of p63 and low levels of EPS8 and CXCL5, while HN12 cells express low levels of p63 (18) and high levels of EPS8 and CXCL5 (3, 18). Previous data show that neither of these cell types expresses functional wt-p53 or mutant p53 (21).

1.12 Hypothesis and Specific Aims

In the current study we propose the following **hypothesis** that GOF mutant p53 enhances expression of CXCL5 by interfering with p63 function in oral cancer cells, and that it cooperates with EGFR/EPS8 signaling to further deregulate chemokine expression, leading to increased cell proliferation and motility. We have identified two specific aims to investigate this hypothesis.

Aim 1 involves the investigation of the role of p63 in regulating expression of CXCL5. In this aim, we will express p63 in oral cancer cells and determine the effect on CXCL5 expression, introduce GOF mutant p53 and p63-specific siRNA into these cells and measure CXCL5 by qRT-PCR and ELISA.

For our second aim, we will investigate the possibility that gain-of-function (GOF) mutant p53 cooperates with EGFR signaling to regulate CXCL5. In this aim, we will co-express EPS8 and mutant p53 in oral cancer cells, and measure CXCL5 mRNA expression. We will also determine the response in terms of CXCL5 expression following EGF treatment of GOF p53-expressing cells.

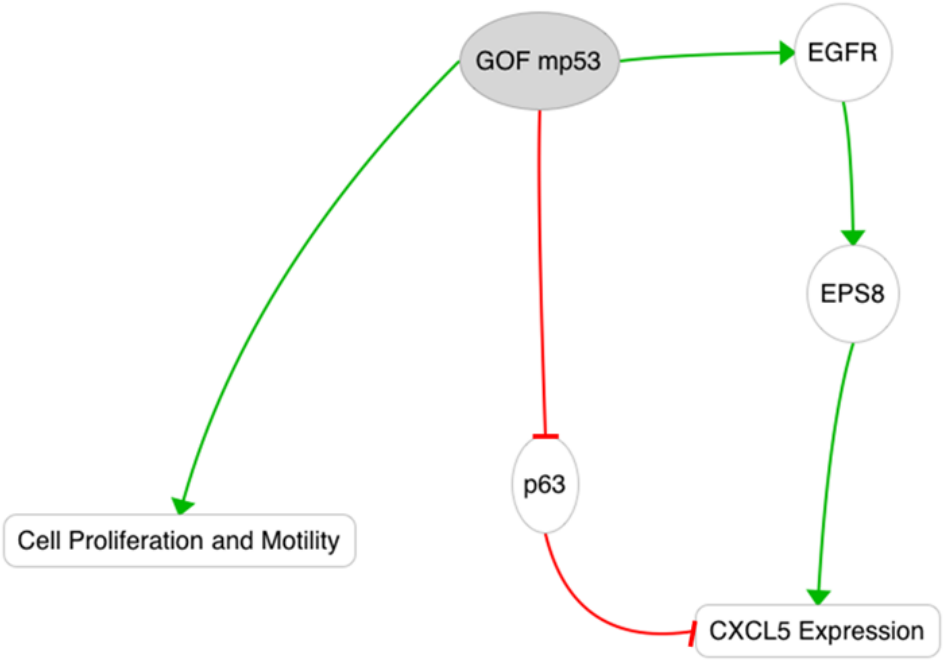

Figure 7. Hypothesis schematic.

Materials and Methods

2.1 Cell Cultures

HN4 cells derived from a primary tongue squamous cell carcinoma and HN12 cells derived from tumor cells that had metastasized to a lymph node from the same patient were maintained in Dulbecco's Modified Eagle's Medium (DMEM) supplemented with 5mL of 100mM sodium pyruvate (Mediatech, Inc.; Manassas, VA), 5mL of 10,000 U/mL penicillin / 10,000 μg/mL streptomycin (Invitrogen; Carlsbad, CA), and 10% fetal bovine serum (FBS). 400μg/mL G418-sulfate or 1μg/mL puromycin-2HCl antibiotic (Enzo Life Sciences, Inc.; Farmingdale, NY) were added to media for cells to be selected for either neomycin or puromycin resistance, respectively. Cells were incubated at 37˚C, 10% CO_2 and the media was changed every 2-3 days.

Before cells grew to confluency, the media was aspirated and the plates were washed with a phosphate buffered saline (PBS) solution to remove any residual growth media. To detatch the cells, 0.1% trypsin-0.88 mM EDTA (Mediatech Inc.; Manassas, VA) was added and the plates were incubated at 37˚C for 5-10 minutes. Cells were then resuspended in 10mL total volume by addition of complete growth medium and re-plated at 1:10 dilution to continue growing.

Cell stocks were made by transferring cells to a 15 mL tube following trypsinization, and centrifuging the cells for 5 minutes at 4˚C. The media was aspirated off,

then cells were resuspended in 1mL of cold Bambanker (Wako Chemicals USA; Richmond, VA), and split between two cryo tubes. The stocks were then stored at -80˚C.

2.2 Plasmids and siRNA

Complementary DNA sequences cloned into mammalian expression plasmid were available in the laboratory. The plasmid containing the ΔNp63α cDNA was obtained from the Oral & Pharyngeal Cancer Branch (NIDCR; Bethesda, MD). All plasmids were verified by sequencing prior to use. Plasmids used were pcDNAIAmp-p53/H179L, which expresses a gain-of-function histidine-to-leucine substitution at codon 179, as described previously (21). pcDNA3-mCherry was obtained from Invitrogen (Carlsbad, CA).

p63 and luciferase siRNAs were synthesized by Sigma-Aldrich, Inc. (St. Louis, MO). The target sequences are shown in Table 1. siRNA duplexes were already annealed by the supplier.

Gene	**Target Sequence**
p63(s)	5’- AACAGCCAUGCCCAGUAUGUA[dT][dT]-3’
p63(as)	5’-UACAUACUGGGCAUGGCUGUU[dT][dT]-3’
Luciferase(s)	5’-CAUGUCAUGUGUCACAUCUC[dT][dT]-3’
Luficerase(as)	5’-GAGAUGUGACACAUGACAUG[dT][dT]-3’

Table 1. siRNA target sequences

2.3 Cell Transfections

Cells were nucleofected (Lonza; Allendale, NJ) using electroporation solution (Mirius Bio; Madison WI) warmed to room temperature and the T-20 protocol, according to the manufacturer's instructions. 1 x 10^6 cells per transfection, as determined using a Cellometer and Cellometer Auto T4 software (Nexelcom Bioscience, LLC.; Lawrence, MA), were resuspended in 100µL electroporation solution and 1µg of the target plasmid DNA was added. In some cases, 1µg mCherry plasmid DNA was added to monitor transfection efficiency by fluorescence microscopy. After transfer to a cuvette and placing the mixture into the Nucleofector II machine (Lonza; Allendale, NJ), the T-20 protocol was run. Cells were then placed into a 10cm plate containing 10mL of media that had been previously warmed in the incubator. After 48 hours, stable cell lines were selected in the presence of either 400µg/mL G418 or 1µg/mL puromycin, depending on the transfected DNA plasmid. For transient siRNA transfections, 1µg of target siRNA was used and cells were harvested after 48 hours without being grown in selection media.

Individual clones from each transfection were isolated by the intensity of fluorescence as viewed using a fluorescent microscope and AxioVision software (Carl Zeiss Microimaging Inc.; Thornwood, NY). Clones were expanded and target gene expression assessed by Western Blot.

2.4 RNA Isolation

1mL of TRIzol reagent (Invitrogen; Carlsbad, CA) was added to each well of sub-confluent cells grown in 6-well plates and incubated on a shaker for 5 minutes at room

temperature to homogenize the samples and ensure nucleoprotein complexes were dissociated. The contents of each well were transferred to sterile 1.5mL microcentrifuge tubes containing 0.2 mL chloroform. Tubes were then shaken vigorously for 15 seconds and centrifuged at 12,000 x *g* for 10 minutes at 4˚C to separate the RNA-containing aqueous phase from the phenol phase. The aqueous phase was then removed and transferred to a new microcentrifuge tube and RNA was precipitated by adding 0.5mL isopropyl alcohol. Tubes were mixed by inverting, and incubated at room temperature for 10 minutes prior to centrifugation for at 12,000 x *g* for 10 minutes at 4˚C. The supernatant was then removed and the RNA pellet was washed with 1mL 75% ethanol. Again, the supernatant was discarded and the pellet dried. RNA was resuspended in 20-30µL RNase-free water and stored at -20˚C. Precautions were taken with each step to avoid sample contamination with RNases to ensure isolation of a pure RNA product.

RNA concentration was measured using a spectrophotometer (Nanodrop; ThermoScientific; Asheville, NC) and ND1000 software. The purity of isolated RNA was assessed by the 260/280 value of each sample, with 260/280 = 2.00 indicating good quality RNA. Additionally, 1µg of RNA was electrophoresed in a 1% agarose gel to confirm sample purity.

2.5 Reverse Transcription

Total RNA was prepared and quantified as previously described, and 1-5µg RNA was added to a microfuge tube along with 1µL each of oligo$(dT)_{18}$ (0.5µg/µL) (Sigma-Aldrich, Inc.; St. Louis, MO) and dNTP mix (10mM each) (Bioline; Taunton, MA). The

volume was made up to 13µL with RNase-free water and the samples were denatured for 5 minutes at 65˚C. After a quick chill on ice followed by a short centrifugation, 4µL 5X First-Strand Buffer (Invitrogen; Carlsbad, CA) and 2µL 0.1M DTT (Invitrogen; Carlsbad, CA) were added to each tube. The microfuge tubes were incubated in a 42˚C water bath for 2 minutes before adding 1µL of MultiScribe reverse transcriptase (50U/µL) (Applied Biosystems; Carlsbad, CA) and mixing gently. Samples were then incubated for 50 minutes at 42˚C to allow the cDNA synthesis reaction to proceed. To inactivate the reaction, tubes were heated at 70˚C for 15 minutes. Samples were stored at -20˚C prior to use as a template for PCR amplification.

2.6 Polymerase Chain Reaction (PCR)

Total RNA was prepared, quantified, and reverse transcribed as previously described. The following reagents were added to 200 µL tubes: 5µL 10X PCR Buffer minus Mg (Invitrogen; Carlsbad, CA), 1µL 10mM dNTP mixture (10mM each), 1.5µL 50mM $MgCl_2$ (Invitrogen; Carlsbad, CA), 1µL of 10µM primer mix (see Table 2), 1µL template cDNA, and 0.2µL Platinum® *Taq* DNA Polymerase (Invitrogen; Carlsbad, CA). RNase-free water was added to make a final reaction volume of 50µL. Samples were mixed and centrifuged briefly before being placed into a GeneAmp PCR System 9700 thermal cycler (Applied Biosystems; Carlsbad, CA). Tubes were incubated at 94˚C for 2 minutes to denature the template DNA and activate the DNA polymerase, followed by 35 PCR amplification cycles: denaturation step at 94˚C for 30 seconds, annealing step at 55˚C for 30 seconds, and extension step at 72˚C for 1 minute. The reaction was then held at 4˚C

and samples were stored at -20˚C until needed for analysis by agarose gel electrophoresis. Oligonucleotide sequences of primers used for PCR were obtained from Sigma-Aldrich, Inc. (St. Louis, MO) and are listed in Table 2.

Gene	**Target Sequence**
p63(s)	5'-GAAACGTACAGGCAACAGCA
p63(as)	5'-GCTGCTGAGGGTTGATAAGC
CXCL5(s)	5'-GTGTTGAGAGAGCTGCGTTG
CXCL5(as)	5'-CTATGGCGAACACTTGCAGA
γ -tubulin(s)	5'-AGAGGGCTTTGTGCTGTGTC
γ -tubulin(as)	5'-ACCAGCTTCTTAGGATACCTG

Table 2. Oligonucleotide sequences for PCR.

2.7 Quantitative Real Time PCR (qRT-PCR)

Total RNA was prepared, quantified, and reverse transcribed as previously described. The following reagents were added to each well of a fast optical 96-well reaction plate (0.1 mL) (Applied Biosystems; Carlsbad, CA): 5µL 2X Blue QPCR SYBR low ROX (Thermoscientific; Epsom, Surrey, UK), 3µL RNase-free water, and 1µL of primer mix (see Table 2). To reduce the chance of error due to pipetting variability, a Master Mix was made containing the previously mentioned reagents for all wells to be used and 9µL of the mix was pipetted into each well. 1µL of template DNA was then added to triplicate wells. As a negative control with no cDNA template, 1µL of RNase-free

water was added to one well per primer mix. 1µL of serial dilutions of previously prepared PCR products for each primer combination were also added to wells to generate relative standard curves for each gene target. The plate was sealed with an RNase-free optical adhesive film (Applied Biosystems; Carlsbad, CA), then centrifuged to collect the samples. The plate was then placed into the 7500 Fast Real-Time PCR System thermal cycler (Applied Biosystems; Carlsbad, CA) and incubated at 50˚C for 2 minutes then 95˚C for 10 minutes before cycling through 40 repetitions of 95˚C for 15 minutes and 60˚C for 1 minute. The amplification cycling was controlled using the 7500 Fast System SDS software.

Tubulin was run with each PCR as a housekeeping gene and used to normalize target gene expression within each sample. The mean value of each primer's triplicate sample wells was calculated and divided by the mean value of the corresponding tubulin wells. Oligonucleotide sequences of primers used for qRT-PCR are listed in Table 2.

2.8 Agarose Gel Electrophoresis

To make a 1% gel, 1g of agarose powder (Bioline; Taunton, MA) was dissolved in 100mL of 0.5X TBE running buffer (45 mM Tris-borate, 1 mM EDTA). The solution was heated in a microwave at 50% power for short intervals to dissolve the agarose and avoid boiling the solution over to ensure the agarose concentration stayed at 1%. 0.5µL of ethidium bromide stain (10µg/µL) was then added to the gel before pouring the cooled solution into a tray with a comb.

Samples were prepared by adding 2.5µL 5X DNA loading buffer (0.25% bromophenol blue, 15% Ficoll 400) to 10µL of PCR product cDNA then loaded into individual wells. Hyperladder I or II molecular weight markers (BioLine; Taunton, MA) were also co-electrophoresed with the samples, depending on the size of the amplified gene fragment. Gels were electrophoresed at a constant 100V for 30 minutes. To visualize bands, the gel was then placed on a UV transilluminator at 302nm and imaged using a CCD camera and software (Alpha Imager, Alpha InnoTec; Germany).

2.9 Protein Isolation

Lysis buffer supplemented with protease inhibitors was prepared by adding 1 µL 10mg/mL leupeptin, 1 µL 10mg/mL aprotinin, and 1µL 0.1M PMSF protease inhibitors to 1mL lysis buffer (10mL of 1M HEPES, pH 7.5; 10mL of 0.5M EGTA, pH 8.0; 4.32 g of 100mM β-glycerophosphate; 5mL of NP-40 lysis buffer; and 625 µL of, 2M $MgCl_2$). Cell lysates were prepared by adding 100µL of lysis buffer to each well of sub-confluent cells grown in six-well plates after washing with cold PBS. Alternatively, 500µL of lysis buffer was added to sub-confluent cells grown in 10cm plates. Prior to the addition of lysis buffer, the plates were washed with cold PBS, which was then thoroughly aspirated. The cells were scraped from the plate and the solution was pipetted into microcentrifuge tubes. The tubes were centrifuged at 4˚C and 10,000RPM for 10 minutes to allow for pellet formation. The clarified protein sample supernatants were removed and kept at -20˚C.

To determine protein concentrations, a standard curve was prepared by making serial dilutions of bovine serum albumin (BSA) (Thermo Scientific HyClone Labs, Inc.;

Logan, UT) in water to determine the absorbance at 600nm visual light for protein concentrations of 50µg/mL, 25µg/mL, 10µg/mL, 5µg/mL, and 1µg/mL. The absorbance was plotted against the concentration and the line of best fit was calculated. This equation was then used to quantify protein samples.

After determining the protein concentration of samples, the amount of protein in the most dilute sample was calculated for a set volume determined by the thickness of the gel to be made. The volume containing the same amount of protein was calculated for all remaining samples and the total volume made up to the original volume. 5X SDS sample buffer (0.25M Tris-HCl pH6.8, 10% SDS, 0.5% bromophenol blue, 50% glycerol, 0.5M DTT) was then added to each sample in microcentrifuge tubes for a final concentration of 1X. The tubes were heated at 100˚C for 10 minutes to denature the proteins. After a quick chill on ice, samples were kept at -20˚C until needed.

2.10 Western Blot Analysis

To determine the amount and molecular size of proteins present in a sample, Western Blotting was used. Cell lysates were prepared and quantified as previously described and electrophoresed on a 1.5 mm thick 10% Tris/glycine SDS-polyacrylamide gel containing 0.1% SDS (36) for 1.5 hours at 110V in 1X SDS-PAGE running buffer (20mM Tris-glycine pH 8.3, 100mM NaCl, 70mM EDTA, 2% (w/v) SDS). Proteins were then transferred to a PVDF transfer membrane (Immobilon-P) (Millipore Corp.; Bedford, MA) overnight in 1X transfer buffer (20mM Tris-HCl pH 7.9, 100mM NaCl, 70mM EDTA, 20% MeOH). Following transfer, the proteins were fixed by placing the membrane

in 100% methanol then allowing it to dry. To rehydrate the membrane, the membrane was placed back into 100% methanol then hydrated in TBS (10 mM Tris HCl pH 7.6, 150 mM NaCl) supplemented with 0.5% Tween 20 (Fisher Bioreagents; Rockville, MD) (T-TBS).

Membranes were washed three times in T-TBS for 10 minutes each then incubated in blocking buffer (5% non-fat dried milk in T-TBS) for one hour on a shaker before incubating overnight at 4˚C in primary antibody recognizing a specific target protein diluted in blocking buffer (Table 3). Membranes were then washed as before in T-TBS and bound antibody was detected by 1 hour incubation at room temperature with the appropriate horseradish peroxidase-conjugated (HRP) secondary antibody diluted in blocking buffer (Table 3). The interaction of primary and secondary antibodies was detected using a mixture of equal parts Western Lightning Oxidizing Reagent Plus and Western Lightning Enhanced Luminol Reagent Plus (PerkinElmer Life Sciences Inc.; Billerica, MA) and imaged using Blue X-ray film (Phenix Research Products; Candler, NC) with a Kodak X-OMAT 2000 Processor.

Primary Antibody	Raised Against	Dilution	Secondary Antibody
p53 (DO-1): sc-126	aa 11-25	1:1,000	Anti-mouse
p53 (FL-393): sc-6243	aa 1-393	1:1000	Anti-rabbit
p63 (4A4): sc-8431	aa 1-205 (ΔN C-terminus)	1:250	Anti-mouse
EPS8	aa 628-821	1:5,000	Anti-mouse
Actin (I-19): sc-1616	C-terminus	1:1,000	Anti-goat

Table 3. Antibodies for Western Blot. All were obtained from Santa Cruz Biotechnology (Santa Cruz, CA) except EPS8, which was obtained from BD Biosciences (San Jose, CA).

2.11 Immunoprecipitation

Cell lysates were first prepared and quantified as described above. 1mg of each sample was placed into a microcentrifuge tube and the volume was adjusted to 1mL with cold lysis buffer. To this, 1μg of antibody per 1mg of the target protein was added and the tubes were placed in a rotator at 4˚C overnight. 30μL of Protein G PLUS-Agarose Immunoprecipitation Reagent (sc-2002; Santa Crus Biotechnology, Inc.; Santa Cruz, CA) was then added to each tube, mixing between each to ensure the packed bead volume was 15μL for all samples. Samples were again placed in a rotator at 4˚C for 50 minutes. The tubes were then centrifuged at 4˚C and 10,000RPM for 10 minutes to collect the beads. The supernatant was quickly poured off and the samples were washed three times with 1mL of cold lysis buffer. Between each wash, the contents of each tube was mixed and centrifuged for 1 minute at 4˚C and 10,000RPM. After the third wash, the lysis buffer was

quickly poured off and samples were again centrifuged for 1 minute. The residual lysis buffer was then carefully removed using a pipette.

To prepare samples for Western Blot, 15µL of lysis buffer was added to the beads to bring the volume back to 30µL for each sample. 6µL of 5X SDS sample buffer was then added to each tube, resulting in a dilution to 1X. Samples were heated at 100˚C for 10 minutes to release the protein from the antibody in addition to denaturing the proteins as previously described. For each immunoprecipitated sample, a corresponding whole-cell sample was also prepared as mentioned in section 2.8 to be included in the Western Blot analysis. After a brief chill on ice, samples were kept at -20˚C until needed.

2.12 Cell Treatment with EGF

Duplicate samples were plated into six-well plates and allowed to attach overnight. The cells were then incubated overnight in 3 mL of 1% serum supplemented with sodium-pyruvate and penicillin-streptomycin as previously described. Epidermal growth factor (EGF) (BD Biosciences; Bedford, MA) was diluted 1:10 in complete growth medium then added to one of each duplicate sample wells to yield a final dilution of 1:1000. The other well was used as a control with no EGF. The plates were incubated for 48 hours and RNA was isolated to be analyzed by QRT-PCR as previously described.

2.13 Wound-Healing (Scratch) Assay

To measure cell motility, the migration of cells into the space of a “wound” administered into a confluent cell monolayer was measured. Cells were plated in triplicate

into 12-well plates and cultured to 100% confluence. One scratch per well was then administered to the center of each well using a sterile pipette tip to create a wound in the monolayer, and the width of the scratch was measured under a 5x objective using a light microscope and AxioVision software (Carl Zeiss Microimaging Inc.; Thornwood, NY). After incubation for 7 hours, the wound width was measured again at the same position. These data were used to calculate the average rate of migration as µm traveled per hour.

2.14 Proliferation Assays

In order to establish cell proliferation rate, cells were first trypsinized and counted as previously described then cells were plated in quadruplicate, at a density of $5x10^3$ cells per well of a 24-well plate. Samples were cultured for seven days and the media was changed every other day. On the final day, 100µL of MTT reagent (5 mg/mL thiazolyl Blue tetrazolium bromide, 98%, in PBS) (Alpha Aesar; Ward Hill, MA) was added to the media and the plates were incubated overnight to allow for crystal formation. The media was then carefully aspirated and 1mL of solublization buffer (10% SDS in 0.01M HCl) was added to each well and the plates were again incubated overnight. A spectrophotometer was used to determine the absorbance of each well using visible light at 570nm, using solublization buffer to blank. Mean absorbance was then calculated for each quadruplicate sample.

Alternatively, on day 7 the cells were detached in 50µL of trypsin then resuspended in 100µL media to make a total volume of 150µL. Cells were counted as previously described and the mean cell number was calculated for each sample.

2.15 Attachment Assay

The attachment efficiency of cells subjected to biological assays was assessed by crystal violet staining (protocol modified from (37)). Cells were seeded in triplicate at a density of 1 x 10^5 cells per well of a 12-well plate and incubated for 1 hour as previously described. The media was removed and cells washed once with PBS, incubated in 0.1% crystal violet in PBS for 5 minutes, and washed 4 times in PBS. 1 mL of 70% ethanol was added to each well to dissolve the stain and absorbance readings were taken at 600nm using a spectrophotometer. 70% ethanol was used as a blank reading. The mean absorbance was then calculated for each sample.

2.16 Collection of Conditioned Media

Cells were seeded in duplicate at a density of 1 x 10^4 cells per well of a 12-well plate and allowed to attach for 24 hours. Cells were then washed with PBS and incubated in serum-free media for 48 hours as previously described. The media was collected and pooled for each sample set and stored at -20˚C. Total cell counts from each well were also determined as previously described and the average cell number calculated for each sample.

2.17 Enzyme-Linked Immunosorbent Assay (ELISA)

To measure the levels of secreted CXCL5 protein, conditioned media was assayed using the DuoSet ELISA Development System (R&D Systems; Minneapolis, MN) and the manufacturer's instructions. 100 µL of CXCL5 capture antibody was added to each well of

a flat-bottom 96-well plate and the sealed plates were incubated overnight at room temperature. The plates were washed four times with 400 µL of Wash Buffer (PBS supplemented with 0.05% Tween 20) (PBS-T) then inverted and blotted against clean paper towels until the wells were completely dry. Plates were blocked using 300 µL of Reagent Diluent (1% BSA in PBS) per well for 1 hour at room temperature then the wash step was repeated as before, ensuring the liquid is completely removed from the plates. 100 µL of conditioned media samples or corresponding dilutions in reagent diluent were added to triplicate wells along with standards and appropriate blanks or controls, sealed, then incubated for 2 hours at room temperature. Standards were prepared by performing serial dilutions of CXCL5 standard, starting at 1:2000 and continuing to 1:7.1825. Reagent diluent was used as a blank and serum-free media was used as a negative control.

The wash step was then repeated as previously mentioned before adding 100 µL of Detection Antibody to each well, sealing the plates as before, and incubating for another 2 hours at room temperature. The plates were again washed and 100 µL of Streptavidin-HRP was added to each well. The plates were sealed and incubated for 20 minutes at room temperature. Additionally, the plates were covered with aluminum foil to reduce exposure to light. After a final wash step, 100 µL of Substrate Solution (1:1 mixture of Color Reagent A (H_2O_2) and Color Reagent B (Tetramethylbenzidine)) was added to each well. Plates were sealed and covered as in the previous step, and incubated for 20 minutes at room temperature. 50 µL of Stop Solution (2N H_2SO_4) was then added to each well to stop the reaction, turning the solution from blue to yellow.

Optical density was measured at 450nm immediately using a microplate spectrophotometer (Epoch; BioTek Instruments; Winooski, VT) and Gen5 software. CXCL5 concentration was calculated from the standard curve. The average was calculated for each sample and normalized to the number of cells per well in each sample as previously measured to determine the amount of CXCL5 secreted per cell.

2.19 Statistical Analysis

Data were analyzed by unpaired t-test to compare two means using GraphPad QuickCalcs software (http://www.graphpad.com/quickcalcs). A p-value less than 0.05 was considered statistically significant.

Results

3.1 HN12 Cells Express Low Levels of p63

It has been previously shown that primary and metastatic tumor cells derived from the same patient have distinctly different levels of chemokine expression (18) and that the transcription factor p63 may contribute to this difference by inhibiting CXCL5 (W.A. Yeudall, unpublished data), so we first wanted to determine the expression level of p63 in our model system. We isolated RNA from HN4 and HN12 cells, reverse transcribed it, then analyzed the cDNA product by qRT-PCR and normalized the results to tubulin as an internal standard. As Figure 8 shows, HN12 cells show a significantly lower level of p63 mRNA expression compared to HN4 cells, which is consistent with published data.

3.2 High CXCL5 Expression in HN12 Cells

We also wanted to confirm the level of CXCL5 expression in our model system, so qRT-PCR was performed using primers specific for CXCL5. As shown in Figure 9, HN12 cells show significantly higher CXCL5 mRNA expression compared to that of HN4 cells, which is consistent with published data (18). Higher expression of CXCL5 observed in HN12 cells coupled with the lower p63 expression raises the possibility of a negative correlation between these two molecules.

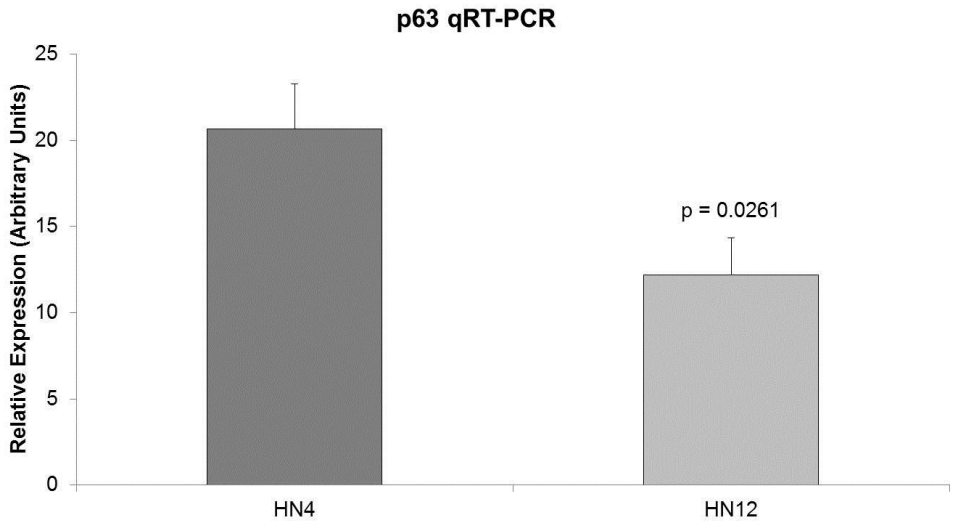

Figure 8. HN12 cells show lower expression of p63 mRNA.
Expression of p63 mRNA in HN4 and HN12 cells as measured by qRT-PCR, normalized to tubulin as a standard. Data are representative of at least three independent experiments. (Bar = S.E.M.)

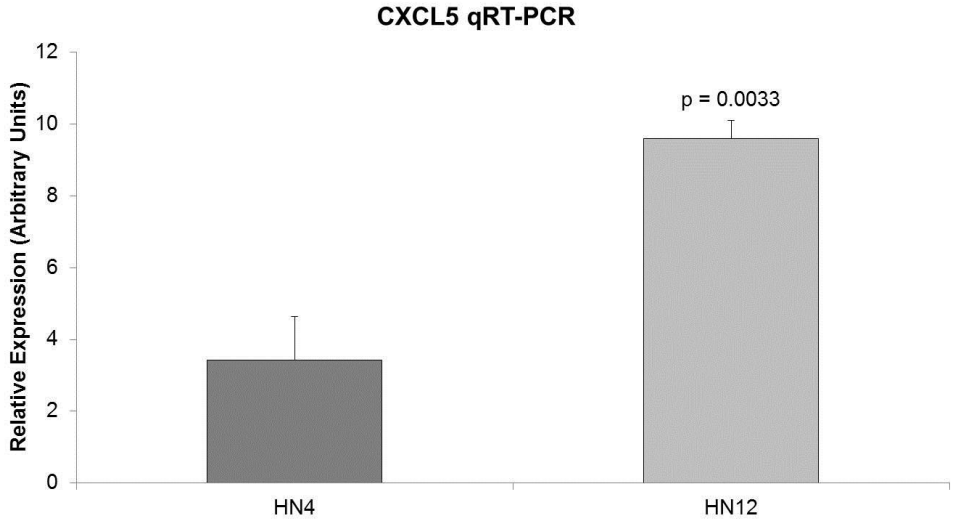

Figure 9. HN12 cells show higher expression of CXCL5 mRNA.
Expression of CXCL5 mRNA in HN4 and HN12 cells as measured by qRT-PCR, normalized to tubulin as a standard. Data are representative of at least three independent experiments. (Bar = S.E.M.)

3.3 Inhibition of p63 Enhances CXCL5 Expression

To next test the hypothesis that p63 inhibits CXCL5 expression, we nucleofected HN4 cells with either small interfering RNA (siRNA) against p63 or with luciferase siRNA as a control. RNA was isolated then cDNA was prepared and analyzed by qRT-PCR. As Figure 10A shows, transfection with p63 siRNA results in inhibition of p63 mRNA expression compared to the control and Figure 10B shows that this inhibition of p63 results in elevated CXCL5 mRNA expression compared to the control. Together with the data showing HN12 cells express low levels of p63 and high levels of CXCL5, these data support the hypothesis that p63 is a negative regulator of CXCL5 expression.

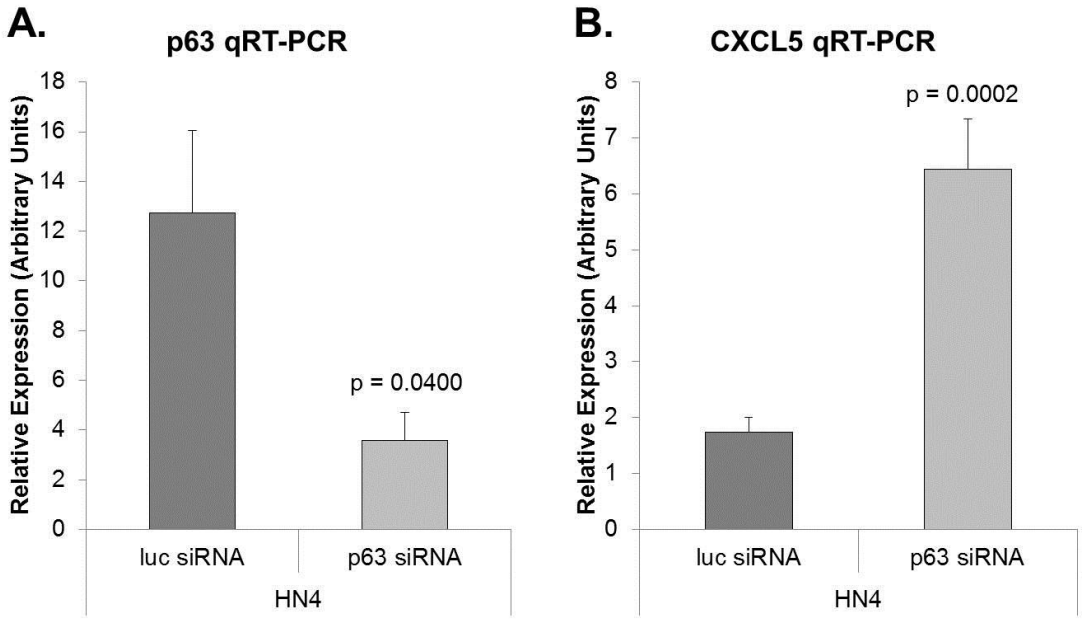

Figure 10. Inhibition of p63 causes an increase in CXCL5 expression.
(A) Expression of p63 mRNA and (B) and CXCL5 mRNA for HN4 cells transfected with either p63 siRNA or luciferase siRNA control, normalized to tubulin as a standard. Data are representative of at least three independent experiments. (Bar = S.E.M.)

3.4 HN4/H179L Cells Express Gain-of-Function Mutant p53

Previous data have shown that gain-of-function (GOF) mutant p53 increases CXCL5 expression in lung cancer cells (20), and that mutant p53 can interact with p63 (24), which our data suggests may be an inhibitor of CXCL5. Because of this, we next wanted to test the contribution of p63 to the mechanism of mutant p53 regulation of CXCL5 expression. HN4 cells were chosen for this model system because they express low levels of CXCL5 and high levels of p63 and we hypothesize that mutant p53 will inhibit the p63 repression of CXCL5 to cause an increase in expression of this chemokine.

We nucleofected HN4 cells with a plasmid encoding the H179L gain-of-function mutant p53, which has a leucine substitution at codon 179, together with neomycin resistance and a plasmid containing the coding sequence for mCherry. As shown in Figure 11, individual G418-resistant clones were selected based on fluorescence intensity as visualized under a fluorescent microscope. Isolated clones were expected to express the target H179L plasmid in addition to the other two selection plasmids. A separate HN4 transfection was also completed with a plasmid containing an empty G418-resistant plasmid as a control.

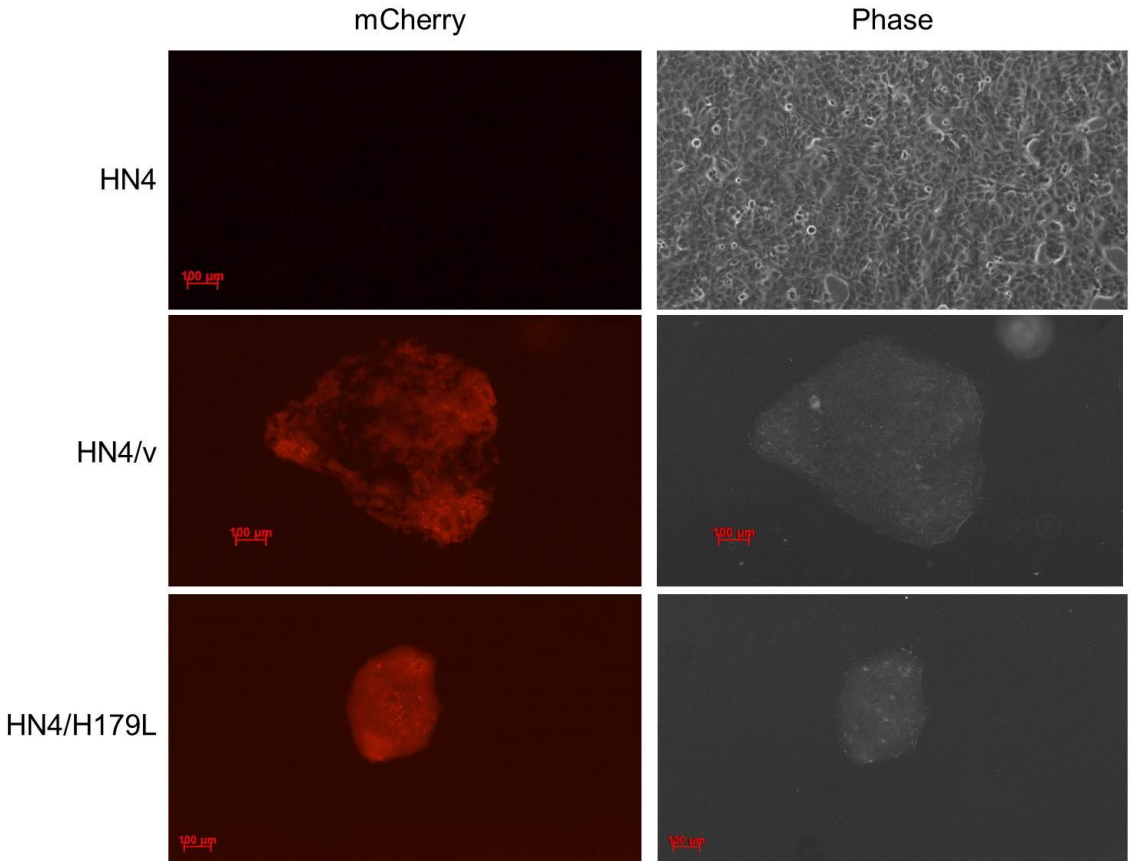

Figure 11. Individual HN4/H179L clones selected for high fluorescence. HN4 cells transfected with a plasmid encoding H179L mutant p53 were also transfected with a plasmid encoding mCherry. HN4/v and HN4 are shown as a control. (5x magnification.)

To determine whether the cells successfully incorporated the H179L plasmid and express mutant p53, cell lysates were prepared and protein expression levels were analyzed by Western Blot. As Figure 12 shows, there are clear p53 bands in the H179L lanes, while these bands are absent in the vector control lanes. The actin bands are shown as an internal control for equal loading across all samples, indicating the observed differences are due to a difference in protein expression and not caused by a change in sample loading. The relative densities were measured, normalized to actin, and are shown below the Western Blot results.

3.5 Mutant p53 Leads to an Increase in CXCL5 Expression

Next, we wanted to determine the effect of mutant p53 on CXCL5 expression, so qRT-PCR was performed and the results are shown in Figure 13. There is a significant increase in CXCL5 mRNA expression in the HN4 cells expressing mutant p53 compared to the empty vector control. This result supports the hypothesis that mutant p53 causes an increase CXCL5 expression, which is consistent with what has been previously found with similar experiments in lung cancer cells (20).

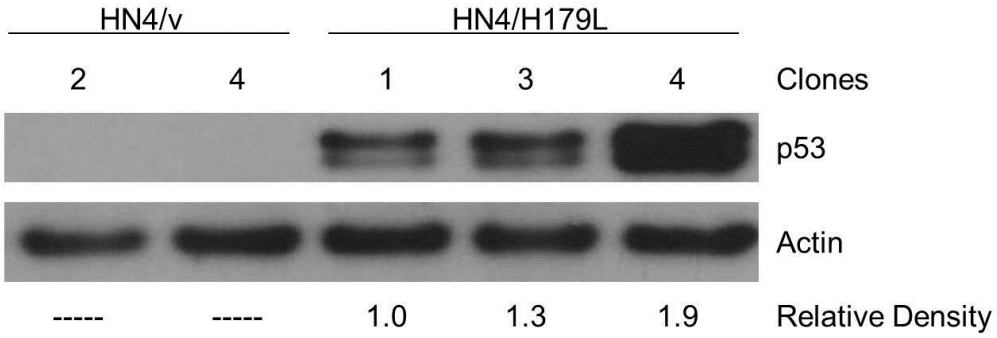

Figure 12. Mutant p53 is expressed in HN4 cells transfected with H179L. p53 protein expression levels were measured for HN4/H179L and vector control clones (top). Actin levels were measured as a control (middle). Relative densities of the p53 bands normalized to actin are also shown (bottom).

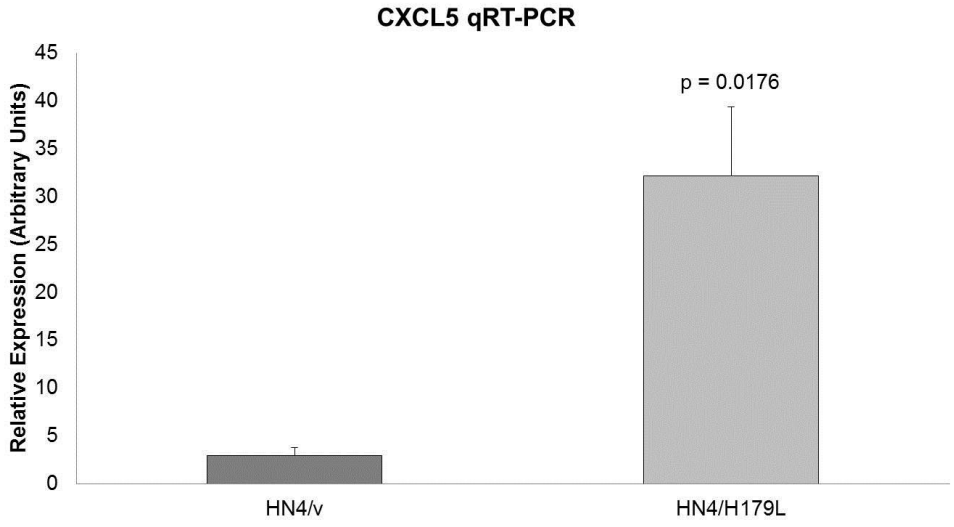

Figure 13. Elevated CXCL5 mRNA expression with mutant p53.
Average expression of CXCL5 mRNA for three individual G418-Selected HN4 clones as measured by qRT-PCR, normalized to tubulin as a standard. An empty vector HN4 transfectant is used as a control. Data are representative of at least three independent experiments. (Bar = S.E.M.)

To complement this observation, conditioned media were collected from each sample of cells seeded at the same density and the level of CXCL5 protein secreted by the cells was measured using an enzyme-linked immunosorbent assay (ELISA) as described in Methods. The results in Figure 14 show that there is a significant increase in the secretion of CXCL5 by the HN4 cells expressing mutant p53 compared to the vector control, which is not unexpected given the similar increase observed for CXCL5 mRNA expression.

3.6 Mutant p53 Does Not Alter p63 mRNA Expression

Next, we wanted to determine what effect, if any, mutant p53 has on p63, so we first tested p63 mRNA levels using qRT-PCR. The results in Figure 15 show that there is not a statistically significant difference in p63 expression between the H179L transfectants and the empty vector control, which indicates mutant p53 does not alter p63 mRNA expression. This result is not unexpected because the presence of mutant p53 has been suggested to alter p63 protein activity (24), not p63 mRNA production.

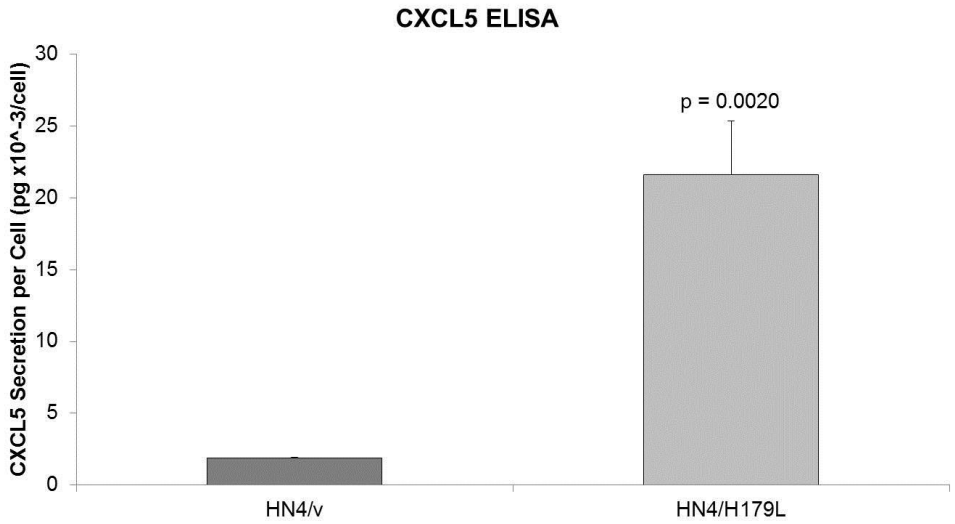

Figure 14. Increased CXCL5 protein secretion with mutant p53.
CXCL5 protein expression in two individual G418-selected HN4 clones expressing mutant p53 as measured by ELISA, normalized to the number of cells per sample. An empty vector HN4 transfectant was used as a control. Data are representative of two independent experiments. (Bar = S.E.M.)

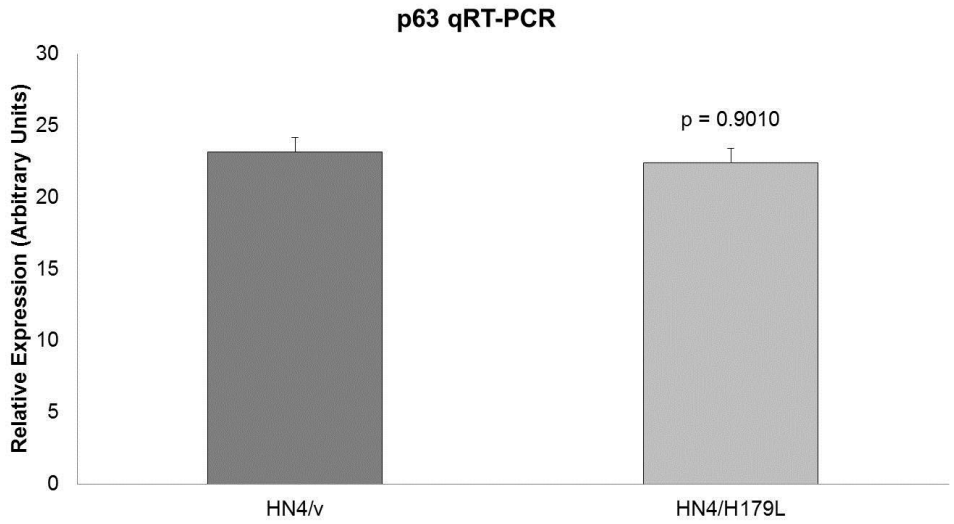

Figure 15. Mutant p53 does not alter expression of p63 mRNA.
Average expression of p63 mRNA for three individual G418-Selected HN4 clones as measured by qRT-PCR, normalized to tubulin as a standard. An empty vector HN4 transfectant was used as a control. Data are representative of at least three independent experiments. (Bar = S.E.M.)

Because p63 mRNA expression levels in the mutant p53 expressing cells are similar to the levels observed for the vector control, any observed changes in CXCL5 expression could be due to the presence of mutant p53. There is also the possibility that mutant p53 is acting to decrease p63 protein levels to cause the observed increase in CXCL5 expression. This is suggested by data shown in Figures 16 and 17, in which the p63 bands for the HN4/H179L cells expressing mutant p53 show reduced density compared to that of the vector control.

3.7 Gain-of-Function Mutant p53 Binds p63

Thus far, we have provided evidence that p63 may be a negative regulator of CXCL5 expression and that inhibition of p63 correlates with increased levels of CXCL5. We have also shown that HN4 cells expressing mutant p53 express elevated levels of CXCL5 compared to the vector control and reduced levels of p63 protein. These two observations taken together suggest that the mechanism by which mutant p53 causes an increase in CXCL5 expression is through interaction with p63 protein, resulting in p63 inhibition.

To assess the interaction between mutant p53 and p63, we immunoprecipitated cell lysates using antibodies specific for p63 as described in Methods, then analyzed the products by Western Blot. Whole-cell lysates were also electrophoresed as a comparison. As shown in Figure 16, p63 bands are visible for the p63 immunoprecipitated samples, indicating successful immunoprecipitation of the target protein. These lanes also show bands when probed for p53, but these 53kD bands overlap the 50kD immunoglobulin

heavy chain bands so these observations are based on the relative densities shown below the Western Blot results. The p53 plus heavy chain bands have increased density compared to the HN4 empty vector control cells that does not express mutant p53 as shown previously in Figure 12 and by the corresponding whole cell lysate lane in Figure 16. We expect that the density of this band must then correspond to the heavy chain alone.

We were able to isolate both p53 and p63 when immunoprecipitating for p63, which suggests these proteins are associated in the cells. Actin and IgG light chain bands are shown as an internal control for equal loading across the whole cell lysate and immunoprecipitated samples, respectively. This indicates that the observed band densities are due to differences in protein expression levels, not due to error in sample loading.

Together, these data suggest that mutant p53 protein interacts directly with p63 to cause an alteration in the normal function of p63. It is proposed that it is through this interaction that mutant p53 prevents p63-induced reduction in CXCL5 expression and that it actually causes an increase in chemokine expression.

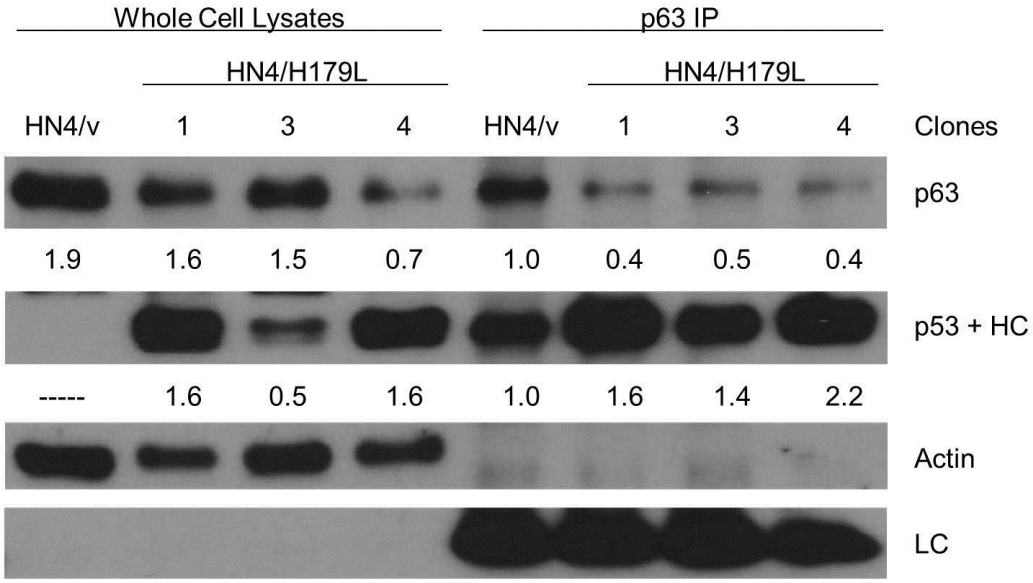

Figure 16. p53 is bound to p63 in HN4 cells transfected with H179L.
Cell lysates were immunoprecipitated with p63-specific antibodies. Whole cell lysate samples are shown as a comparison. Actin and immunoglobulin light chain levels are shown as a control. Relative densities of the p63 and p53 bands normalized to actin for whole cell lysates, or normalized to light chain for IPs are also shown.

3.8 Inhibition of p63 Enhances CXCL5 Expression in the Presence of Mutant p53

So far our data suggest that the mechanism by which mutant p53 increases CXCL5 expression in our model system is through inhibition of p63, so we next wanted to determine what effect inhibition of p63 would have on CXCL5 expression in these cells. We nucleofected our model system cells with either p63 siRNA or luciferase siRNA as a control, then confirmed downregulation of p63 protein expression by p63 siRNA by preparing cell lysates and analyzing them by Western Blot. As Figure 17A&B show, cells transfected with p63siRNA do not express detectable p63, whereas p63 bands are observed in the control luciferase siRNA transfectant lanes. This indicates that the siRNA successfully interfered with expression of the p63 gene, both for the cells expressing mutant p53 and the empty vector control cells.

Our previous data showed that inhibition of p63 in the parental HN4 cells results in enhanced CXCL5 expression, so we next wanted to determine the effect of p63 inhibition on CXCL5 expression in the presence of mutant p53. We hypothesized that mutant p53 acts by interfering with the p63 repression of CXCL5 expression, so we would expect further inhibition of p63 to cause an even higher increase in CXCL5. As the results in Figure 18 show, for both the mutant p53-expressing HN4 cells and the vector control, inhibition of p63 results in an increase in CXCL5 expression compared to the luciferase siRNA control, which is consistent with our previous results implicating p63 as a negative regulator of CXCL5. Additionally, the increase in CXCL5 expression in the HN4/v/p63 siRNA cells in response to p63 inhibition is significantly higher than that observed in the HN4/H179L/luc siRNA control cells, almost reaching the expression levels of HN4/H179L

cells with p63 inhibited. This may suggest that mutant p53-mediated inhibition of p63 function is inefficient compared to siRNA-mediated downregulation, or that mutant p53 elevates chemokine expression by two (or more) mechanisms: one dependent on p63 and one independent. These two observations together suggest that inhibition of p63 alone may be sufficient to cause an increase in CXCL5 expression, which points to p63 as a crucial mediator in the mechanism of p53 regulation of this chemokine.

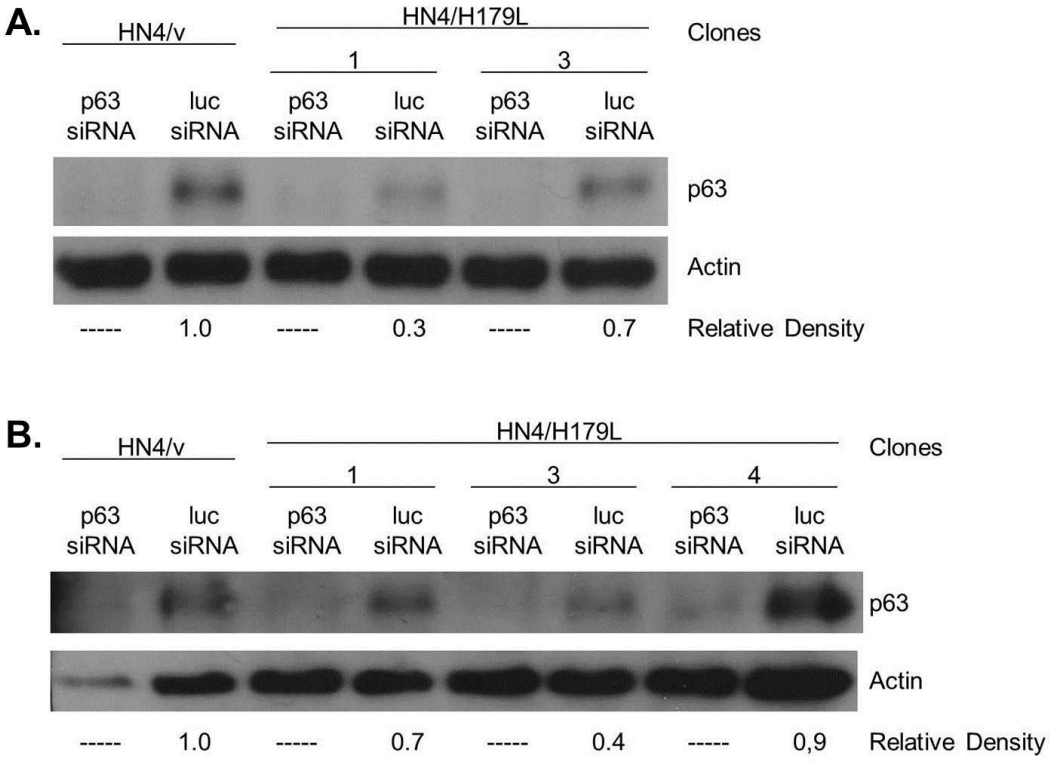

Figure 17. Successful inhibition of p63 expression with p63 siRNA.
p63 expression in HN4 cells expressing mutant p53 and the vector control transfected with either p63 or luciferase siRNA (top). Actin levels were measured as a control (middle). Relative densities of the p63 bands normalized to actin are also shown (bottom). (A) and (B) correspond to two separate siRNA transfection experiments.

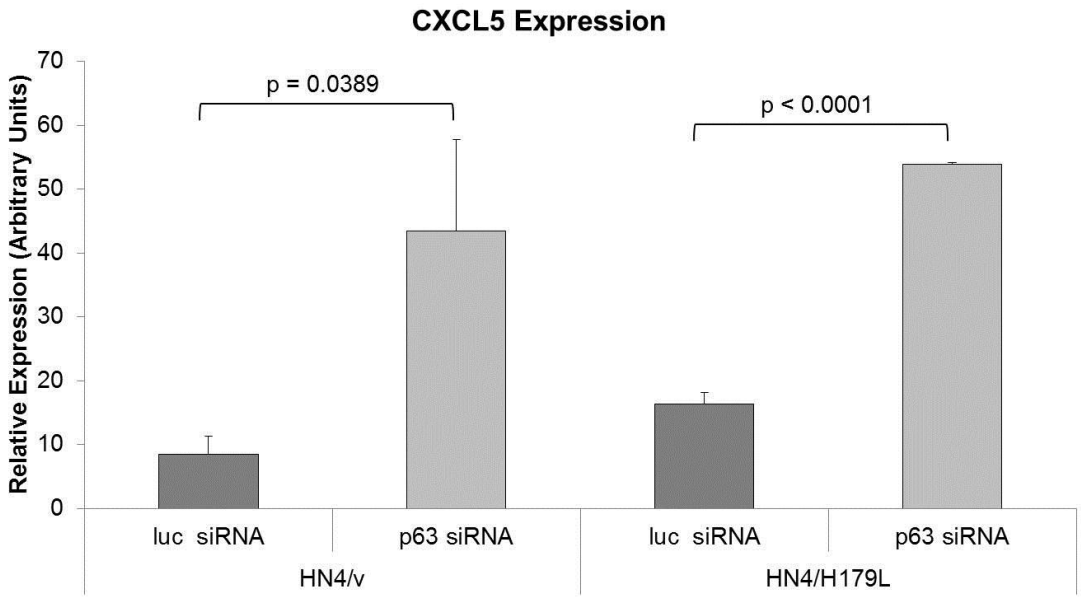

Figure 18. Inhibition of p63 causes an increase in CXCL5 expression. Expression of CXCL5 mRNA for mutant p53 expressing HN4 cells transfected with either p63 siRNA or luciferase siRNA control, normalized to tubulin as a standard. Empty vector control is shown as a comparison. Data are representative of at least three independent experiments. (Bar = S.E.M.)

3.9 Mutant p53 Increases Proliferation and Motility

To determine the significance of the CXCL5 mRNA and protein expression data obtained thus far, biological experiments were performed because mutant p53 has also been linked to cell migration and proliferation in cancer (18, 20). Additionally, reduced p63 expression has been linked to increased tumor cell invasion and metastasis (25) and our cells expressing mutant p53 also show reduced levels of p63 expression.

First, to determine the effect of mutant p53 on cell motility, a wound-closure (scratch) assay was performed. The cells were plated in triplicate into 12-well plates and grown to 100% confluence, a "wound" was made with a pipette tip, and the width of the denuded region was measured at 0h then 7h, as shown in Figure 19. These data were used to calculate the rate of migration and the results are shown in Figure 20. Cells transfected with mutant p53 show a significant increase in migration rate compared to that of the vector control cells, which is consistent with published data (20).

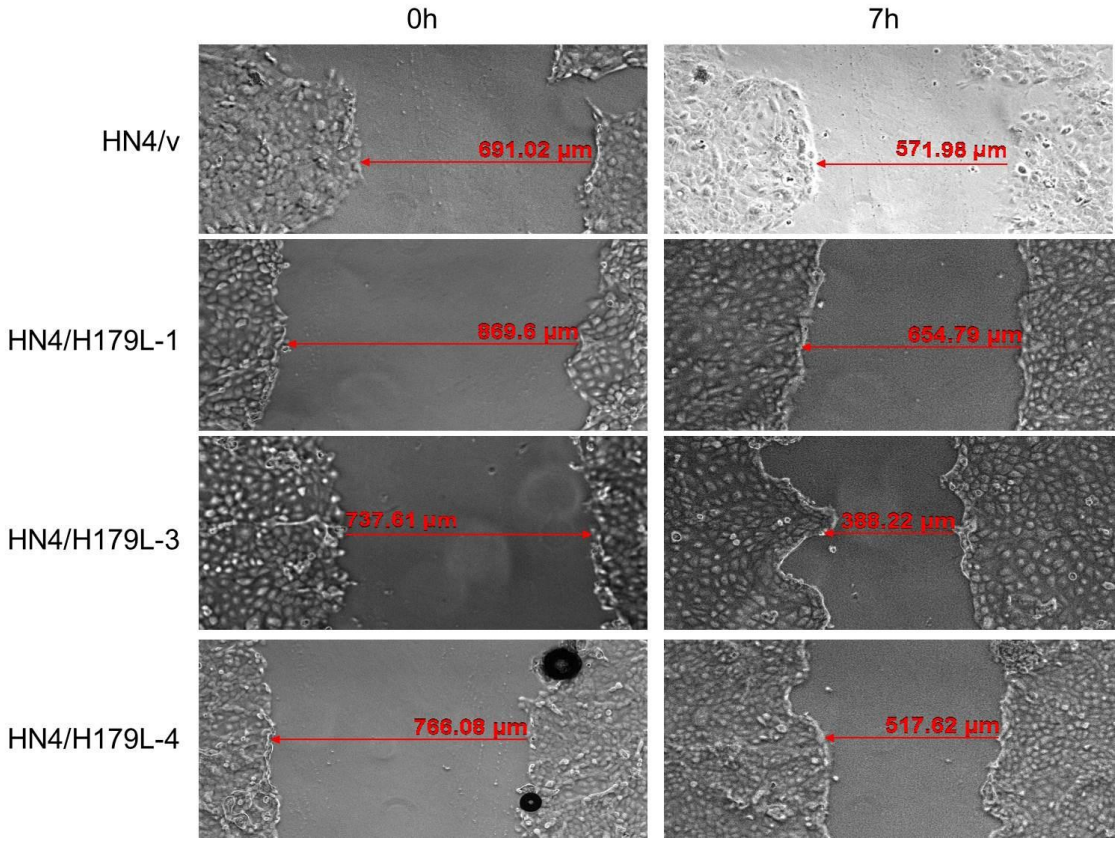

Figure 19. "Scratch" width measured at 0h and again at 7h.
HN4/v and HN4/H179L cells were subjected to wound closure assay, as described in the Methods. Migration rate was calculated by dividing the distance migrated by the time. Data were obtained by 12 independent measurements, and are representative of at least three independent experiments. (5x magnification.)

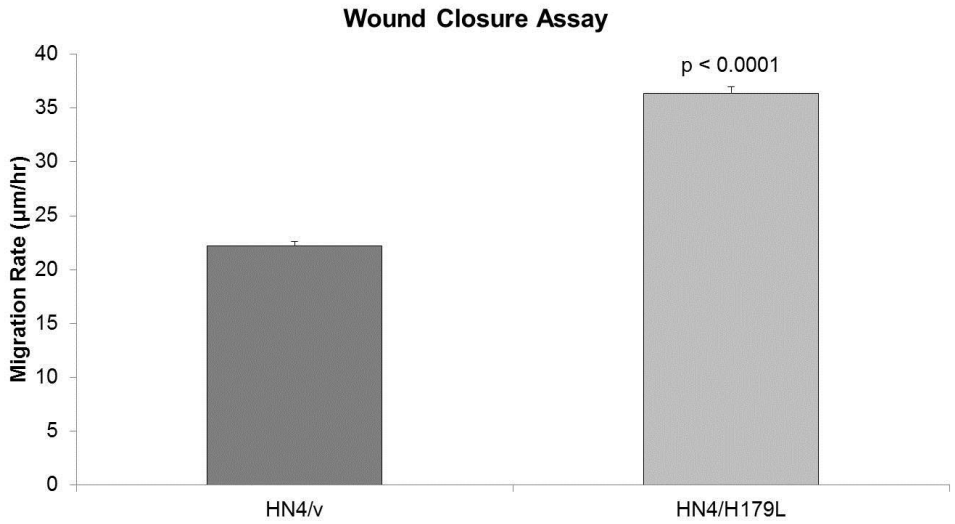

Figure 20. Enhanced cell migration with mutant p53.
Average distance traveled as measured by the Scratch Assay. An empty vector HN4 transfectant is used as a control for the HN4H179L transfectants. Data are representative of at least three independent experiments. (Bar = S.E.M.)

CXCL5 has also been shown to enhance cell proliferation (18), so to test this in the presence of mutant p53, cells were seeded at $5x10^3$ cells per well in quadruplicate in 24-well plates and cultured for seven days. At that point, either an MTT assay was performed by first adding MTT reagent to crystalize the cells overnight then dissolving the crystals in solublization buffer to measure the absorbance, or the cells were counted. The results are shown in Figure 21. For both assays, the cells expressing mutant p53 show a significant increase in proliferation compared to the empty vector control. Again, this supports the hypothesis that mutant p53 enhances cell proliferation.

To confirm that these results showing the HN4 cells expressing mutant p53 have increased proliferative capacity are due to the increase in CXCL5 and not to an acquired advantage that allows for increased plating efficiency, an attachment assay was performed. As the results in Figure 22 show, the cells expressing mutant p53 do not have a significant attachment advantage, but there is still a 1.8-fold increase in cell attachment with the HN4/H179L cells compared to the vector control. This suggests that the increase in proliferation observed in the HN4 cells expressing mutant p53 is due to increased cell growth rates but the increased plating efficiency cannot be completely ruled out as a contributing factor.

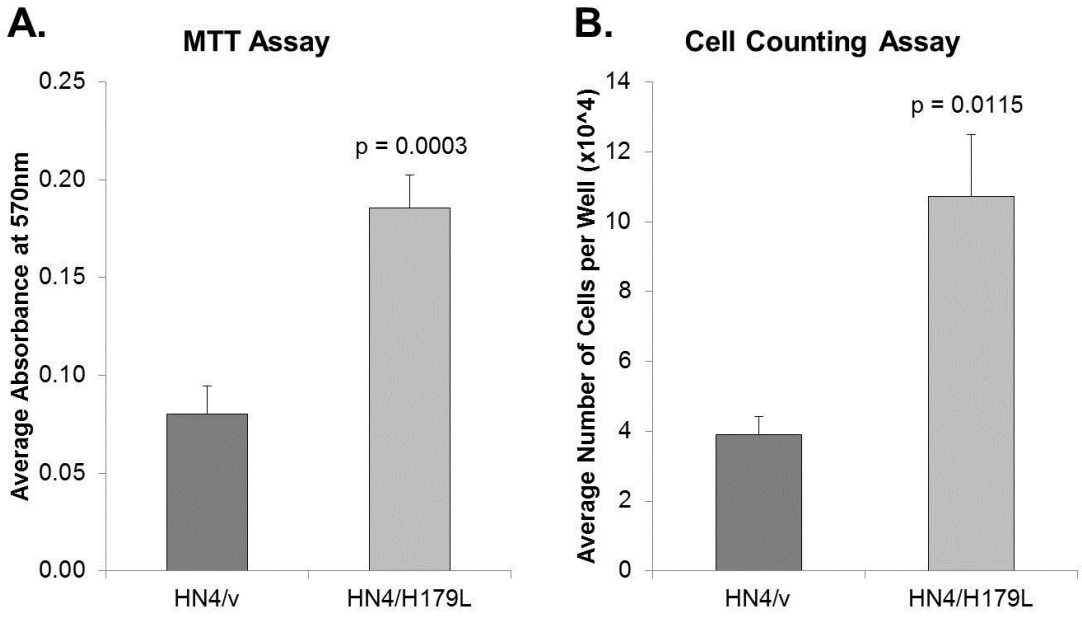

Figure 21. Increased proliferation with mutant p53.

Average absorbance as measured by (A) MTT Assay or (B) average number of cells per well, after 7 days. Cells were seeded at a density of $5x10^3$ cells/mL. An empty vector HN4 transfectant is used as a control. Data are representative of at least three independent experiments. (Bar = S.E.M.)

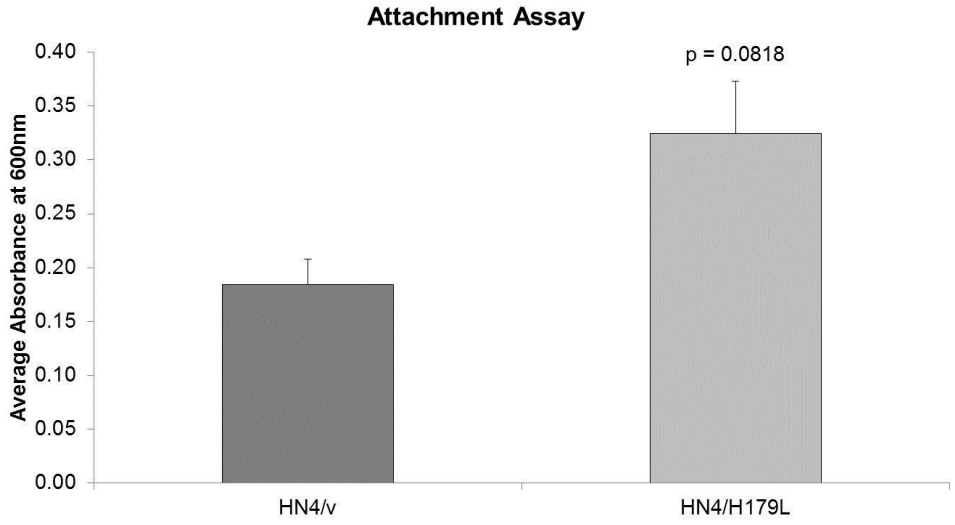

Figure 22. No attachment advantage with mutant p53.
Average absorbance as measured by crystal violet attachment assay as described in Methods, after 1 hour. Cells were seeded at a density of $1x10^3$ cells/well. An empty vector HN4 transfectant is used as a control. Data are representative of at least three independent experiments. (Bar = S.E.M.)

3.10 HN4/H179L Cells Display Increased CXCL5 Expression in Response to EGF

Previous studies have shown that another mechanism by which CXCL5 expression is increased in tumor cells is through stimulation of epidermal growth factor receptor (EGFR) signaling (3). We hypothesized that mutant p53 cooperates with this EGF pathway to further increase chemokine expression so to test this in our cells expressing mutant p53, we treated cells with EGF. RNA was isolated for reverse transcription and the cDNA product was analyzed by qRT-PCR with primers specific for CXCL5. Cells were grown in 1% serum media alone as a control.

As the results in Figure 23 show, cells expressing mutant p53 show a statistically significant increase in CXCL5 mRNA expression when treated with EGF compared to the no EGF control, which still shows higher CXCL5 expression than the vector control cells with and without EGF treatment. This result is expected if mutant p53 and EGF act via independent pathways to increase CXCL5 expression in a cooperative manner.

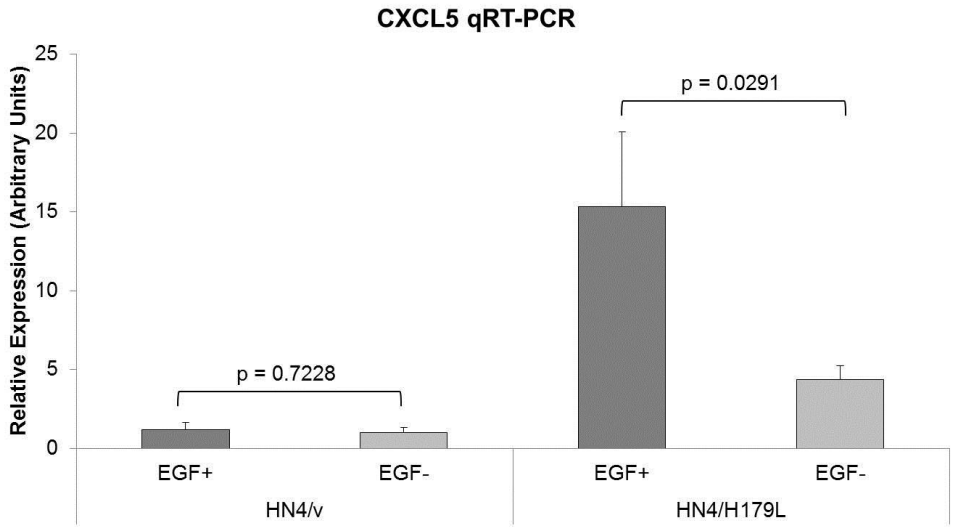

Figure 23. Cooperative increase in CXCL5 with mutant p53 plus EGF. Expression of CXCL5 mRNA in G418-selected HN4 clones in the presence and absence of EGF treatment as measured by qRT-PCR, normalized to tubulin as a standard. An empty vector HN4 transfectant as used as a control. Data are representative of at least three independent experiments. (Bar = S.E.M.)

3.11 HN4/EPS8/H179L Cells Express Both Mutant p53 and EPS8

Our data thus far suggests that mutant p53 cooperates with the EGFR pathway to increase CXCL5 mRNA expression, so we next wanted to evaluate the role of the downstream EGFR pathway mediator, EPS8 (15), in this regulation. Previously transfected HN4 cells that overexpress EPS8 and possess puromycin-resistance were transfected with a plasmid containing the gene encoding for the H179L p53 mutant plus G418-resistance and mCherry. As a control, HN4/H179L cells were transfected with an empty vector encoding the gene for puromycin resistance and HN4/EPS8 cells were transfected with an empty vector encoding the G418-resistance gene. These cells were grown in media containing both G418 and puromycin to select only for the cells that express both of these antibiotic resistance plasmids. Figure 24 shows phase-contrast microscope images.

To assess whether the HN4/EPS8 cells successfully incorporated the mutant p53 plasmid, cell lysates were prepared and analyzed by Western Blot and the results are shown in Figure 25. Actin bands are shown as an internal control for equal loading across all samples and the relative densities are also shown, normalized to actin. The HN4/EPS8/H179L cells show bands for both p53 and EPS8, indicating successful co-expression of these two plasmids, but the expression levels of each are lower than would be expected given the band densities of the controls. The EPS8 band is half as dense when co-expressed with mutant p53 compared to the HN4/EPS8/v control and the p53 band shows a similar reduction in density compared to that of the HN4/H179L/v control. Interestingly, the HN4 cells expressing the mutant p53 plasmid alone have increased EPS8

expression compared to the HN4 empty vector control, raising the possibility that mutant p53 increases EPS8 expression.

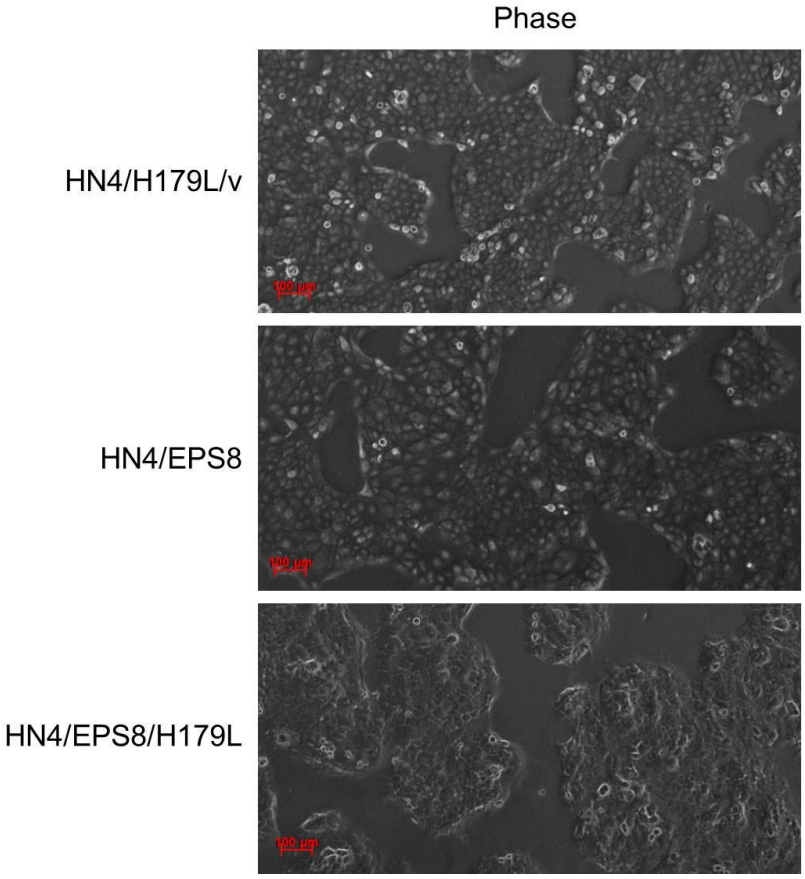

Figure 24. HN4 cells co-transfected with H179L and EPS8.
HN4 cells expressing EPS8 were transfected with a plasmid encoding H179L mutant p53. HN4/EPS8/v and HN4/H179L/v are shown as a control. (5x magnification.)

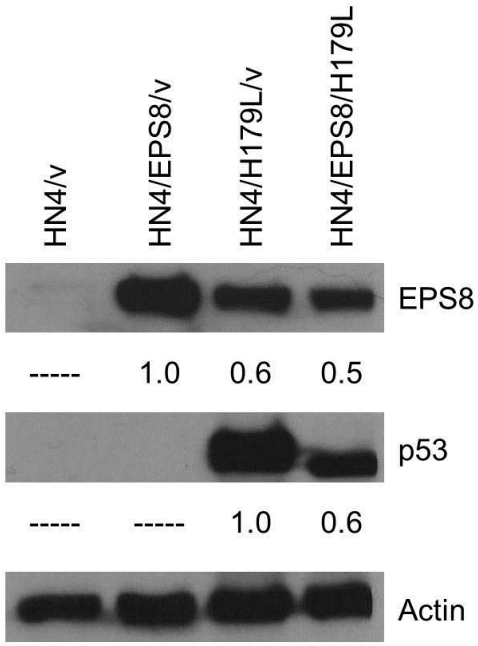

Figure 25. HN4/EPS8/H179L cells express both mutant p53 and EPS8. EPS8 protein expression levels were measured for HN4/v, HN4/EPS8/v, HN4/H179L/v, and HN4/EPS8/H179L cells (top). Actin levels were measured as a control (middle). Relative densities of the bands normalized to actin are also shown (bottom).

3.12 Mutant p53 and EPS8 Cooperate to Increase CXCL5 Expression

Next, we wanted to determine what effect co-expression of EPS8 and mutant p53 would have on the expression levels of CXCL5 mRNA, so we performed qRT-PCR and the results are shown in Figure 26. HN4 cells overexpressing EPS8 show an increase in CXCL5 that is consistent with published data (35) and the HN4 cells co-expressing mutant p53 and EPS8 show CXCL5 expression that is slightly higher than with EPS8 alone. The HN4 cells expressing the H179L mutant p53 plasmid and show a resulting increase in EPS8 expression show the highest expression of CXCL5 mRNA. These data taken together suggest that mutant p53 and EPS8 may function in a cooperative manner to increase expression of CXCL5.

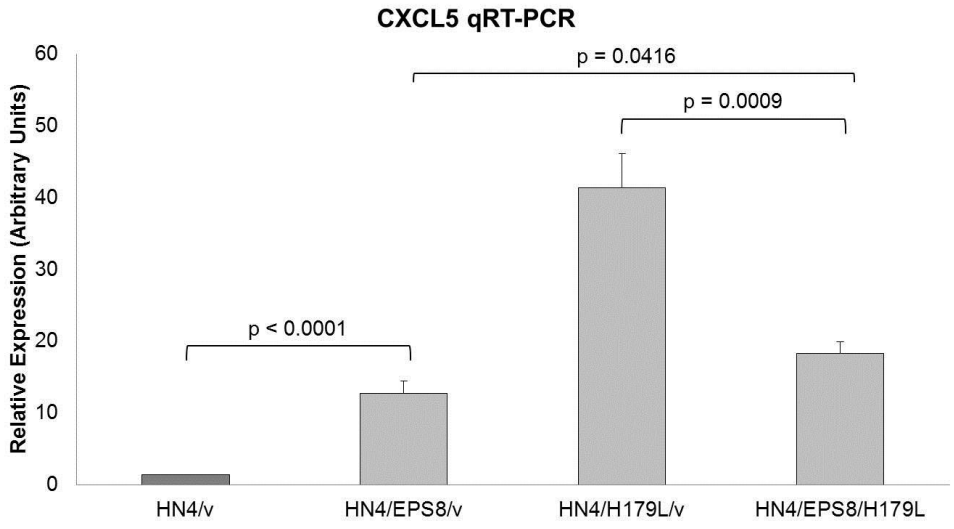

Figure 26. EPS8 and mutant p53 cooperate to increase CXCL5.
Average expression of CXCL5 mRNA in selected G418-/puromycin-selected HN4 cells as measured by qRT-PCR, normalized to tubulin as a standard. Empty vector HN4/H179L and HN4/EPS8 transfectants were used as a control. Data are representative of at least three independent experiments. (Bar = S.E.M.)

Discussion

4.1 Mutant p53 Enhances HNSCC Tumorigenesis

Previous studies have shown that gain-of-function (GOF) mutant p53 increases expression of the CXC-chemokine, CXCL5 (20), which has been linked to increased tumor cell motility and proliferation (18). Mutant p53 has also been shown to favor tumorigenesis through enhancement of tumor cell migration and proliferation (20), but the exact mechanisms have yet to be fully understood. Several possible mechanisms have been postulated through which mutant p53 can increase CXCL5 expression, including inhibition of its family member, p63 (24), direct binding of the CXCL5 promoter region to activate gene expression (20), or mutant p53 activation of NF-κB2 (20) or other transcription factors yet to be identified. Thus far, mutant p53 has not been localized on the CXCL5 promoter using ChIP assays. As others have suggested that some mutant p53 gain-of-function activity is mediated by interfering with p63 function (24), in this study we investigated whether GOF mutant p53 enhances expression of CXCL5 by interfering with p63 function in oral cancer cells.

In the current study, we utilized HN4 tongue primary tumor cells transfected with the H179L gain-of-function mutant p53 as a model system to study the effect of mutant p53 on CXCL5 expression. After confirming mutant p53 expression by Western Blot, we showed an 11-fold increase in CXCL5 expression using both qRT-PCR and ELISA in the

HN4 cells expressing mutant p53 compared to the empty vector control. We were able to induce significantly higher levels of CXCL5 expression by expressing mutant p53 in HN4 cells that normally express very low levels of this chemokine, as shown by both transcript levels and amount of secreted protein.

We were also able to show that when HN4 cells express mutant p53, these cells respond with an almost 2-fold increase in cell migration, as measured by wound closure assays. Because of the increased levels of chemokines secreted by the HN4/H179L cells, this increase in migration could be due to the more concentrated chemokine gradient created by these cells. The cells would then be attracted toward the gradient at a faster rate than for the control cells that are not exposed to this same gradient and normally show low levels of migration. It is also possible that the mechanism is not via CXCL5-induced motility, and further experiments using inhibition of the CXCR2 receptor or downstream mediators could be utilized to confirm the role of this chemokine in cell migration.

Additionally, proliferation assays showed mutant p53 caused up to a 3-fold increase in cell growth. HN4 cells normally proliferate slowly and we were able to demonstrate that expression of mutant p53 in these cells induces an increase in this biological process that is important for tumor progression. We also performed attachment assays, which suggest that when HN4 cells express mutant p53 they may have an advantage that allows for increased attachment efficiency when plating, although the results were not statistically significant. Further studies should be completed to determine whether this attachment advantage is only observed when plating, or if this acquired phenotype plays a role with tumor progression to possibly favor colonization of a

secondary tumor site during metastasis. Additional experiments are also needed to determine whether the observed increase in cell proliferation by HN4 cells expressing mutant p53 is the result of increased CXCL5 expression, or if there is another mechanism that is responsible.

The results of these studies are significant because they confirm previous lung cancer studies that show it only takes a single missense mutation in the p53 protein to induce a more metastatic phenotype (21). This is even more concerning because of the increased risk for p53 mutations associated with tobacco use (6) and the low five-year survival rate associated with metastasized tumors (3). Figure 27 shows the possible interactions between these molecules to induce the altered biological responses observed.

Although we did not explore this in the current study, it would be interesting to also compare the results of HN4 cells expressing mutant p53 with HN12 cells derived from a metastasized lymph node tumor.

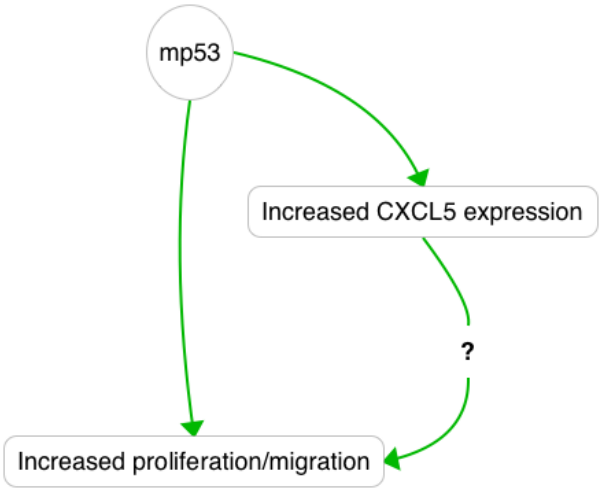

Figure 27. Mutant p53 promotes HNSCC tumorigenesis.

4.2 p63 is a Negative Regulator of CXCL5 Expression Inhibited by mp53

Preliminary studies from our laboratory have suggested that inhibition of p63 correlates with an increase in CXCL5 expression in lung cancer cells. In the present study, we found a profound increase in CXCL5 expression in HN4 oral cancer cells transfected with p63 siRNA. This raises the possibility that p63 inhibition may be a contributory event to tumor progression that is common across different types of cancers. Additionally, we were able to show a similar upregulation of CXCL5 with siRNA inhibition of p63 in HN4 cells expressing mutant p53. These cells already showed elevated levels of CXCL5 expression and using siRNA against p63, we were able to elevate it further.

HN4/H179L showed lower p63 protein levels but no significant change in p63 mRNA, which suggests this decrease is not transcriptionally mediated. It may instead be possible that mutant p53 leads to increased turnover of the p63 protein, although this has not been reported previously. Decreasing p63 mRNA further using siRNA may be responsible for the enhanced levels of CXCL5 over and above those seen in the presence of mutant p53. Alternatively, it may be that mutant p53 activates CXCL5 expression by mechanisms other than (or in addition to) p63 inhibition. Also, the CXCL5 expression in the HN4/H179L cells transfected with p63 siRNA or luciferase control siRNA are still significantly higher than the corresponding HN4/v cells. This also suggests there may be an additional p63-independent mechanism by which mutant p53 increases CXCL5 expression because regardless of the p63 status, the mutant p53-expressing cells express higher CXCL5.

Previous studies have shown that p53 interacts with p63 to inhibit its function (24), so we sought to investigate this p63-dependent regulation of CXCL5 expression further. Our results suggest two possible ways through which mutant p53 inhibits p63, which are illustrated in Figure 28. One possibility is that mutant p53 causes a decrease in p63 protein, which reduces the inhibition on CXCL5 enough to cause the increase in CXCL5 expression but it is also likely that this is mediated by direct protein interaction. By binding p63, mutant p53 could inhibit the function of p63 as a transcriptional repressor of CXCL5. When immunoprecipitating p63, we were able to co-precipitate p53 as well, which suggests that these proteins are bound in the cells. Together with the decreased levels of p63 measured in the HN4 cells expressing mutant p53, this adds evidence to suggest that mutant p53 binding p63 may have two effects: one to one to decrease the total p63 protein levels by targeting the molecule for degradation and another to inhibit p63 via direct binding. This two-fold inhibition of p63 protein expression and function could together result in the observed increase in CXCL5 expression in our model system.

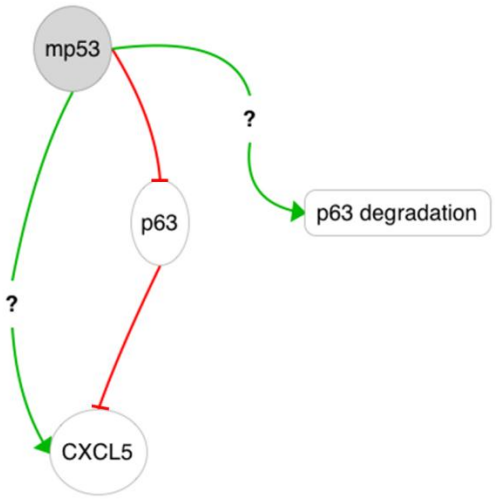

Figure 28. Two possible p63-dependent mechanisms of mutant p53 regulation of CXCL5 expression.

In addition to our HN4/H179L mutant p53 model system, we also investigated CXCL5 expression with upregulation of p63 in HN12 cells and these results are shown in Appendix A. HN12 cells normally express low levels of p63 and high levels of CXCL5 (18), so our expectation was that by increasing p63 levels in these cells there would be a corresponding decrease in CXCL5 expression. Unfortunately, we were unsuccessful in elevating the levels of p63 in these cells, but the unexpected result was that following transfection, these cells actually showed a decrease in p63 expression with a corresponding increase in CXCL5 expression compared to the empty vector control. This result also supports the hypothesis that p63 acts to inhibit the expression of CXCL5. Previous studies have shown that overexpressing p63 may result in growth arrest and apoptosis (7), which may offer an explanation as to why this approach was not successful. If the cells that successfully incorporated the p63 plasmid underwent apoptosis, that could leave a

surviving population that only express lower levels of p63. This could account for our observed decrease in p63 expression and corresponding CXCL5 increase.

4.3 Mutant p53 and EGFR Signaling Cooperate to Elevate CXCL5

Previous studies have also implicated EGFR-dependent signaling pathways as another mechanism by which CXCL5 is increased in cancer, possibly through the downstream regulator, EPS8 (35). Previous data have shown that treatment of cells with EGF stimulates CXCL5 expression along with other genes that favor metastasis (3) and it was also found that overexpression of EPS8 causes an increase in CXCL5 expression (35).

We hypothesized that mutant p53 cooperates with the EGFR signaling pathway to further increase the expression of CXCL5. When treating HN4 cells expressing mutant p53 with EGF, we were able to show a 3.5-fold increase in CXCL5 expression compared to cells with no EGF treatment, while the vector control HN4 cells showed a less pronounced change in CXCL5 expression. Our data have shown that mutant p53 expression alone acts to elevate the expression of CXCL5 in our model system, and upon activation of the EGFR signaling pathway with EGF ligand, the expression of CXCL5 is elevated further. If mutant p53 and EGFR act through the same pathway to activate CXCL5 expression, we would not expect to see this increase in CXCL5 expression, so this suggests that these pathways act through independent mechanisms to cooperatively increase the expression of CXCL5.

We have already demonstrated a link between mutant p53 and p63, and there are previous data that also link p63 and EGFR. These studies show that treatment with EGF

causes decreased p63 expression, but also shows an increase in ΔNp63α-induced motility (10, 34). This seems to be conflicting evidence, but there are several possible explanations. It could be the fact that these results come from studies performed with different cell types, and p63 expression levels may be cell type-specific. Another possible explanation is that reduction of total p63 levels could allow for a more profound effect of one specific isoform. The decrease in p63 could be caused by a reduction in only some isoforms, while others could still be upregulated while maintaining the same level of total p63. Further studies should be completed with our model system to determine the expression levels of the individual p63 isoforms in our model system to more specifically identify the role that p63 plays in tumor progression.

Taken together with our data showing upregulation of CXCL5 expression in cells expressing mutant p53 when treated with EGF, these studies suggest that inhibition of p63 may also play a role in this increase. By further inhibiting p63 expression to alleviate repression of CXCL5 in our cells, EGFR signaling pathways may be promoting elevation in CXCL5 expression. Another possibility is that expression of the EGFR is upregulated by mutant p53. If the cells express more of the receptor, the effect of treatment with EGF ligand would be more pronounced in the HN4/H179L cells than in the HN4/v control cells. This is consistent with our observations so in addition to further experiments to evaluate p63 levels, effects on EGFR expression should also be determined.

We next sought to show a similar effect by co-transfecting HN4 cells with EPS8 and mutant p53. We were able to successfully transfect both expression plasmids into HN4 cells; however, this resulted in lower levels of expression as compared to the single

transfectants, which was unexpected. Interestingly, when testing for EPS8 using Western Blot, we noticed an elevation in the expression levels of EPS8 in the HN4/H179L/v cells, compared to the HN4 control. This was not expected given the EPS8 levels expressed by the HN4/v cells, and raises the possibility that mutant p53 may also regulate EPS8. This could be yet another mechanism by which mutant p53 elevates CXCL5 expression in these cells. To further test this, the levels of EPS8 expression for our individual HN4/H179L clones could be measured to determine whether these cells also express detectable EPS8.

When we measured CXCL5 expression levels, HN4 cells expressing EPS8 showed an increase in CXCL5 that we would expect given published data (15), and the HN4 cells expressing mutant p53 showed CXCL5 elevation similar to the data we observed in our previous results. We were unable to show a synergistic increase in CXCL5 expression in our co-transfectant model, but this does not necessarily mean that these two pathways act independently. Table 4 shows the relative expression of EPS8, mutant p53, and CXCL5 in this model system. The HN4 cells expressing both mutant p53 and EPS8 showed approximately half of the mutant p53 expression than the HN4/H179L/v, while both express similar levels of EPS8. These EPS8 levels, however, are approximately half that of the HN4/EPS8/v cells, which showed the lowest increase in CXCL5 expression. The HN4/EPS8/H179L cells showed a slightly higher level of CXCL5 despite showing half the EPS8 expression of HN4/EPS8/v. The slight increase in CXCL5 expression could be due to the presence of mutant p53, which raises the possibility that if these cells expressed higher EPS8 or mutant p53, they would also express higher levels of CXCL5. This is actually shown by the HN4/H179L/v cells, which was unexpected. These cells express

similar levels of EPS8 as the HN4/EPS8/H179L cells, but express almost double the level of mutant p53, which correlates to a little over 2-fold increase in CXCL5 expression.

	HN4/v	**HN4/EPS8/v**	**HN4/H179L/v**	**HN4/EPS8/H179L**
EPS8	---	1.0	0.6	0.5
p53	---	---	1.0	0.6
CXCL5	0.1	1.0	3.2	1.4

Table 4. Relative Expression of EPS8, p53, and CXCL5.

Together with our findings with EGF treatment, these data also suggest a cooperative function between these two pathways. These results are significant because like mutant p53, EGFR is also overexpressed in many cancers (15), and this pathway has been shown to favor tumor progression (33). If these two pathways that independently promote tumorigenesis actually work together to amplify the expression of CXCL5, they could reduce the time it takes for a tumor to progress and metastasize to distant sites in the body. Additional studies could be done to further determine the degree to which cooperativity occurs and confirm whether the EPS8 downstream mediator plays a role. For example, the effect on CXCL5 expression could be evaluated in response to inhibition of EPS8 using siRNA. Alternatively, the levels of the EPS8 downstream mediator, FOXM1 (35), could also be measured in our model system. Most importantly, the effect of this cooperativity on the biological processes important for tumor progression should be evaluated.

4.4 Limitations of the Current Study

Although our *in vitro* model has offered an effective way to study HNSCC, there are still limitations that should be taken into consideration. Because these cells are grown in culture, they are not exposed to all of the different factors that are present in the body. We do try to mimic body conditions by controlling the temperature and humidity of the environment in which our cells are grown, and by supplementing the cell culture media with growth factors, but the current study should be continued to an *in vivo* model to complement the results we have obtained thus far.

Another assay we utilized was the wound closure, or scratch, assay. Although this is an effective way to measure the migration rates of cells in culture, it is a two-dimensional model and an additional study would be to repeat the experiment using a trans-well migration assay to measure motility through a three-dimensional matrix. This would be more representative of what actually occurs in the body. Another limitation to the wound closure assay is that the width of the initial scratch might influence migration rate because of the CXCL5 gradient produced by the cells. This could also affect the migration rates, especially for the cells expressing mutant p53 that secrete elevated levels of this protein. This experiment was repeated multiple times and the results were averaged to reduce any effect this might have had on the calculated migration rates.

We were able to utilize MTT and cell counting assays to test the proliferative capacity of our cells; however there are some disadvantages to these methods. Both MTT and cell counting assays depend on plating the correct initial densities of cells for all samples, so even slight differences in the starting concentration may affect the final result.

Plating the cells at a higher initial density could give the cells a growth advantage which could be interpreted as increased proliferation. Another limitation to the cell counting assay is that by using a Cellometer and cell counting program, there is the possibility that concentrations could be incorrectly measured. If the cells were not properly resuspended and separated, a grouping of cells could be counted as only one which would result in inaccurate concentration results. Also, the presence of dead cells on the slide could contribute to altered concentration that could skew the results. To avoid this, we were careful to properly resuspend cells and to limit the time between trypsinization and cell counting to avoid cell death.

4.5 Future Studies

The future direction of this line of study should ultimately continue to animal *in vivo* studies, but additional *in vitro* experiments could also be done. To further complement the migration data we have obtained thus far, invasion assays could also be performed to determine whether mutant p53 induces a more invasive phenotype in our model system. Luciferase assays and chromatin immunoprecipitation (ChIP) assays could also be completed to determine the effect of mutant p53 or EGFR inhibition of p63 on the CXCL5 promoter. Luciferase assays could be used to determine the activity of the promoter and ChIP assay would show whether the promoter is in an active form or if p63 is bound. The goal of further *in vitro* experimentation should be to elucidate the mechanism by which mutant p53, p63, and EGFR signaling function to regulate the expression of CXCL5; and what impact this has on tumor progression. Finally, the role of individual p63

isoforms in the overall function of p63 in our model system should be tested to determine what isoforms contribute to the tumorigenic phenotype.

4.6 Conclusions

The results of the current study indicate a role for mutant p53 in head and neck squamous cell carcinoma proliferation, migration, and tumorigenicity, possibly through enhancement of CXCL5 expression. The results support the hypothesis that GOF mutant p53 enhances expression of CXCL5 by interfering with p63 function in oral cancer cells, and that mutant p53 cooperates with EGFR/EPS8 signaling to further deregulate chemokine expression. Figure 29 shows the possible interactions between these molecules that result in increased expression of CXCL5 and altered biological responses. Further research can be conducted to determine the extent of the role played by p63 in mutant p53 regulation of CXCL5 in tumorigenicity and the extent of the cooperativity between EGFR signaling and mutant p53.

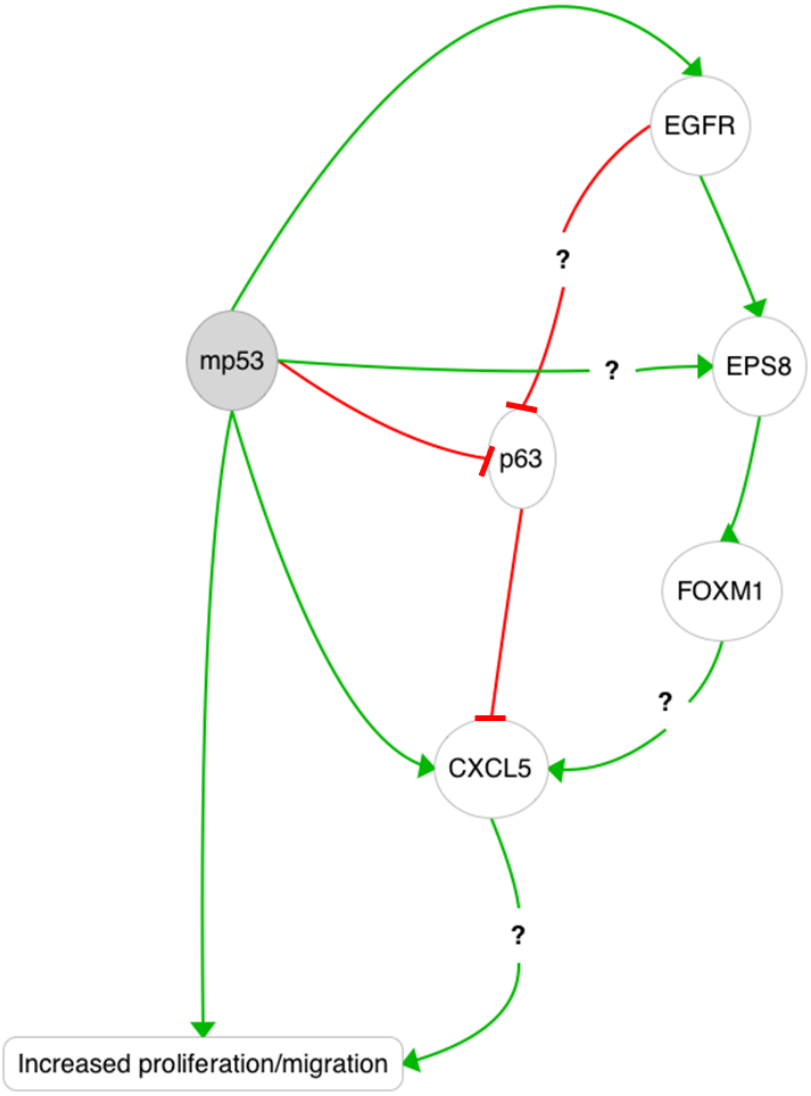

Figure 29. Possible interactions between mutant p53, p63, and EGFR.

Literature Cited

Literature Cited

1. Lim YC, Oh S, Cha YY, Kim S, Jin X, Kim H. Cancer stem cell traits in squamouspheres derived from primary head and neck squamous cell carcinomas. Oral Oncol. 2011;47(2):83-91.

2. Yeudall WA, Miyazaki H. Chemokines and squamous cancer of the head and neck: Targets for therapeutic intervention? Expert Rev Anticancer Ther. 2007;7(3):351-60.

3. Miyazaki H, Patel V, Wang H, Ensley JF, Gutkind JS, Yeudall WA. Growth factor-sensitive molecular targets identified in primary and metastatic head and neck squamous cell carcinoma using microarray analysis. Oral Oncol. 2006;42(3):240-56.

4. Ragin CCR, Modugno F, Gollin SM. The epidemiology and risk factors of head and neck cancer: A focus on human papillomavirus. J Dent Res. 2007;86(2):104-1.

5. Schlecht NF, Franco EL, Pintos J, Negassa A, Kowalski LP, Oliveira BV, et al. Interaction between tobacco and alcohol consumption and the risk of cancers of the upper aero-digestive tract in brazil. Am J Epidemiol. 1999;150(11):1129-37.

6. Ronchetti D, Neglia CB, Cesana BM, Carboni N, Neri A, Pruneri G, et al. Association between p53 gene mutations and tobacco and alcohol exposure in laryngeal squamous cell carcinoma. Arch Otolaryngol Head Neck Surg. 2004;130:303-6.

7. Barbieri CE, Pietenpol JA. p63 and epithelial biology. Exp Cell Res. 2005;312(6):695-706.

8. Pai SI, Westra WH. Molecular pathology of head and neck cancer: Implications for diagnosis, prognosis, and treatment. Annu Rev Pathol. 2009;4:49-70.

9. Ha PK, Chang SS, Glazer CA, Califano JA, Sidransky D. Molecualr techniques and genetic alterations in head and neck cancer. Oral Oncol. 2009;45(4-5):335-9.

10. Danilov AV, Neupane D, Nagaraja AS, Feofanova EV, Humphries LA, DiRenzo J, et al. DeltaNp63alpha-mediated induction of epidermal growth factor receptor promotes pancreatic cancer cell growth and chemoresistance. PLoS ONE. 2011;6(10):1-15.

11. Shin DM, Kim J, Ro JY, Hittleman J, Roth JA, Hong WK, et al. Activation of p53 gene expression in premalignant lesions during tumorigenesis. Cancer Res. 1994;54:321-6.

12. Benke EM, Ji Y, Patel V, Wang H, Miyazaki H, Yeudall WA. VEGF-C contributes to head and neck squamous cell carcinoma growth and motility. Oral Oncol. 2010;46(4):e19-24.

13. Bazley LA, Gullick WJ. The epidermal growth factor receptor family. Endocrine-Related Cancer. 2005;12:S17-2.

14. Christofakis EP, Miyazaki H, Rubink DS, Yeudall WA. Roles of CXCL8 in squamous cell carcinoma proliferation and migration. Oral Oncol. 2008;44:920-6.

15. Wang H, Patel V, Miyazaki H, Gutkind JS, Yeudall WA. Role for EPS8 in squamous carcinogenesis. Carcinogenesis. 2008;30(1):165-74.

16. Munoz LM, Holgado BL, Martinez-A C, Rodriquez-Frade JM, Mellado M. Chemokine receptor oligomerization: A further step toward chemokine function. Immunol Lett. 2012;145(1-2):23-9.

17. Vinader V, Afarinkia K. The emerging role of CXC chemokines and their receptors in cancer. Future Med Chem. 2012;4(7):853-67.

18. Miyazaki H, Patel P, Wang H, Edmunds RK, Gutkind JS, Yeudall WA. Down-regulation of CXCL5 inhibits squamous carcinogenesis. Cancer Res. 2006;66(8):4279-84.

19. Vinader V, Afarinkia K. A beginner's guide to chemokines. Future Med Chem. 2012;4(7):845-52.

20. Yeudall WA, Vaughan CA, Miyazaki H, Ramamoorthy M, Choi M, Chapman CG, et al. Gain-of-function mutant p53 upregulates CXC-chemokines and enhances cell motility. Carcinogenesis. 2012;33(2):442-51.

21. Yeudall WA, Jakus J, Ensley JF, Robbins KC. Functional characterization of p53 molecules expressed in human squamous cell carcinomas of the head and neck. Molec Carcinogen. 1997;18(2):89-96.

22. Nishi H, Senoo M, Nishi KH, Murphy B, Rikiyama T, Matsumura Y, et al. p53 homologue p63 represses epidermal growth factor receptor expression. J Biol Chem. 2001;276(45):41717-24.

23. Wrighton KH, Prele CM, Sunters A, Yeudall WA. Aberrant p53 alters DNA damage checkpoints in response to cisplatin: Downregulation of CDK expression and activity. Int J Cancer. 2004;112(5):760-7.

24. Melino G. p63 is a suppressor of tumorigenesis and metastasis interacting with mutant p53. Cell Death Differ. 2011;18(9):1487-99.

25. Barbieri CE, Tang LJ, Brown KA, Pietenpol JA. Loss of p63 leads to increased cell migration and up-regulation of genes involved in invasion and metastasis. Cancer Res. 2006;66(15):7589-97.

26. Zaika E, Wei J, Yin D, Andl C, Moll U, El-Rifai W, et al. p73 protein regulates DNA damage repair. FASEB J. 2011;25:4406-14.

27. Nylander K, Vojtesek B, Nenutil R, Lindgren B, Roos G, Zhanxiang W, et al. Differential expression of p63 isoforms in normal tissues and neoplastic cells. J Path. 2002;198(4):417-2.

28. Matheny KE, Barbieri CE, Sniezek JC, Arteaga CL, Pietenpol JA. Inhibition of epidermal growth factor receptor signaling decreases p63 expression in head and neck squamous carcinoma cells. Laryngoscope. 2003;113:936-9.

29. Boldrup L, Coates PJ, Gu X, Nylander K. dNp63 isoforms regulate CD44 and keratins 4, 6, 14, and 19 in squamous cell carcinoma of head and neck. J Path. 2007;213(4):384-91.

30. Boominathan L. The tumor suppressors p53, p63, and p73 are regulators of MicroRNA processing complex. PLoS ONE. 2010;5(5):1-11.

32. Yen C, C Y, Pan C, Lu K, Chen PC, Hsia J, et al. Copy number changes of target genes in chromosome 3q25.3-qter of esophageal squamous cell carcinoma: TP63 is amplified in early carcinogenesis but down-regulated as disease progressed. World J Gastroenterol. 2005;11(9):1267-72.

33. Normanno N, De Luca A, Bianco C, Strizzi L, Mancino M, Maiello MR, et al. Epidermal growth factor receptor (EGFR) signaling in cancer. Gene. 2006;366(1):2-16.

34. Kubo T, Ichimiya S, Tonooka A, Nagashima T, Kikuchi T, Sato N. p63 induces CD4+ T-cell chemoattractant TARC/CCL17 in human epithelial cells. J Interferon Cytokine Res. 2008;28:725-32.

35. Wang H, Teh M, Ji Y, Patel V, Firouzabadian S, Patel AA, et al. EPS8 upregulates FOXM1 expression, enhancing cell growth and motility. Carcinogenesis. 2010;31(6):1132-41.

36. Sambrook J, Russel DW. Molecular cloning: A laboratory manual. New York: Cold Spring Harbor Laboratory Press; 2001.

37. Fahraeus R, Lane D. The p16INK4a tumor suppressor protein inhibits avB3 integrin-mediated cell spreading on vitronectin by blocking PKC-dependent localization of avB3 to focal contacts. Embo J. 1999;18(8):2106-18.

APPENDIX A

Reduced p63 Expression in HN12 Cells Transfected with ΔNp63α

We have shown that inhibiting p63, whether by siRNA or through mutant p53 interference, results in an increase in CXCL5 expression, so we wanted to explore this further. HN12 cells expressing low levels of p63 and high levels of CXCL5 were nucleofected with both a plasmid containing the ΔNp63α isoform plus G418-resistance and mCherry. We selected individual clones grown in G418-supplemented media based on the intensity of fluorescence fluorescence as visualized under a fluorescent microscope, shown in Figure 30. As with our previous clone selections, the assumption was that if the cells incorporated the mCherry plasmid, they also incorporated the ΔNp63α plasmid. A separate transfection was completed with a plasmid containing an empty G418-resistant plasmid as a control.

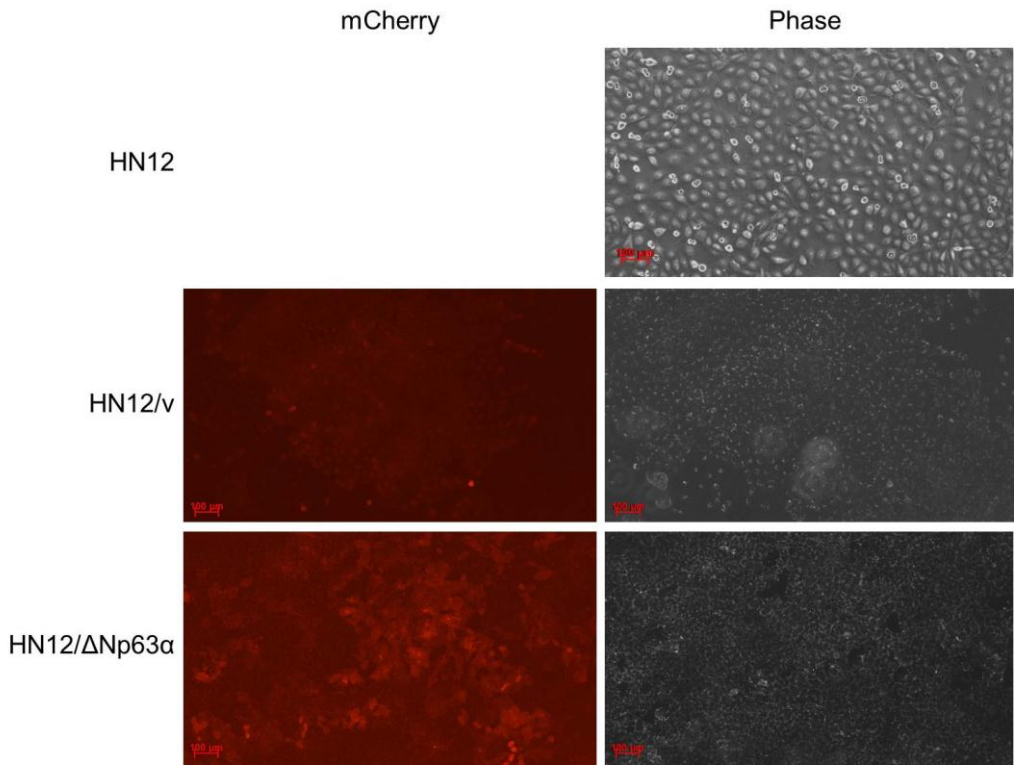

Figure 30. Individual HN12/ΔNp63α clones selected for high fluorescence. HN12 cells transfected with a plasmid encoding ΔNp63α were also transfected with a plasmid encoding mCherry. Colonies were selected for high fluorescence. HN12/v and HN12 are shown as a control.

To determine whether the HN12/ΔNp63α transfections were successful in upregulating p63 expression, protein lysates were prepared and analyzed by Western Blot. As Figure 31 shows, the p63 band is stronger in the empty vector control lane than in the lane for HN12/ΔNp63α. Actin bands are shown as an internal control and the relative densities are shown below the Western Blot results. This was not the expected result, so p63 mRNA levels were also measured using qRT-PCR and the results shown are an average for four separate clones. As Figure 32 shows, p63 mRNA expression levels are reduced in the ΔNp63α transfectants compared to the vector control, which is consistent with the Western Blot results. Together, these data show that there is an unexplained downregulation of p63 by the HN12 cells upon transfecction of the ΔNp63α isoforms.

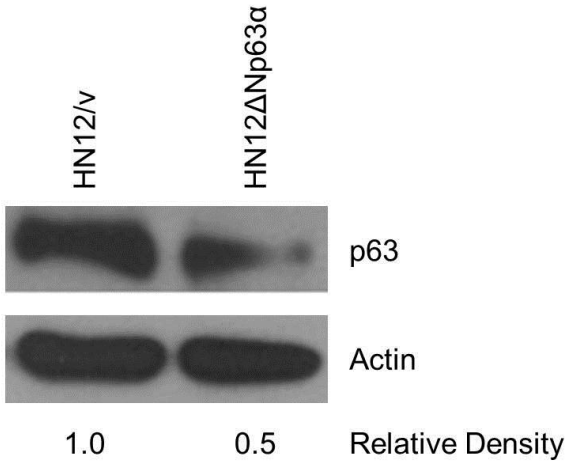

Figure 31. Reduced p63 protein expression in HN12/ΔNp63α cells.
p63 protein expression levels were measured for HN12/ΔNp63α and vector control clones (top). Actin levels were measured as a control (middle). Relative densities of the p53 bands normalized to actin are also shown (bottom).

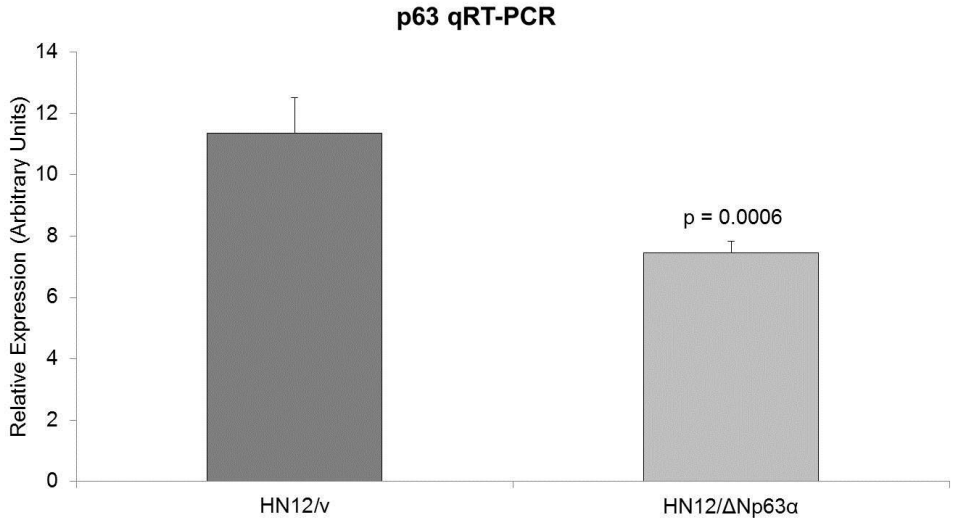

Figure 32. Reduced p63 mRNA expression in HN12/ΔNp63α cells. Expression of p63 mRNA in four separate G418-selected HN12 clones as measured by qRT-PCR, normalized to tubulin as a standard. An empty vector HN12 transfectant was used as a control. Data are representative of at least three independent experiments. (Bar = S.E.M.)

Increased CXCL5 with Reduced p63 Expression

Although the HN12/ΔNp63α transfections did not yield desired overexpression of p63, we still wanted to evaluate the effect on CXCL5 expression given that the results have so far show that a decrease in p63 expression causes an increase in CXCL5. In order to test this, qRT-PCR was completed with primers specific for CXCL5. As Figure 33 shows, there is a significant increase in CXCL5 expression in the HN12/ΔNp63α cells compared to the empty vector control, which is consistent with our previous findings. A similar increase was observed for CXCL5 protein secretion, as measured by ELISA, and these results are shown in Figure 34. Although the observed increase in CXCL5 expression in the cells showing decreased p63 expression supports the hypothesis that p63 is involved with repression of CXCL5, our ultimate goal was to overexpress p63 and because we were unsuccessful no further experiments were done using this approach.

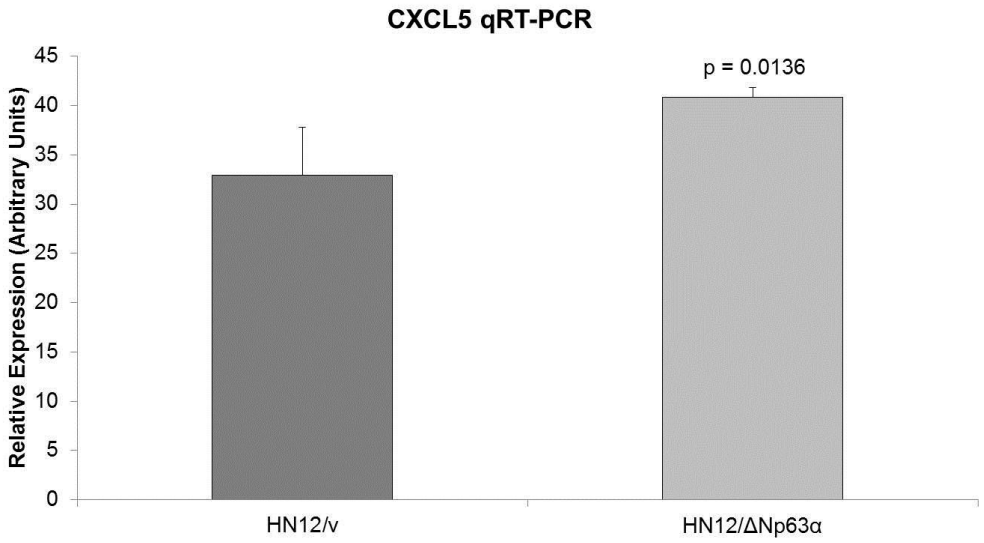

Figure 33. Reduced p63 correlates with elevated CXCL5 mRNA.
Average expression of CXCL5 mRNA for four individual G418-selected HN12 clones as measured by qRT-PCR, normalized to tubulin as a standard. An empty vector HN12 transfectant was used as a control. Data are representative of at least three independent experiments. (Bar = S.E.M.)

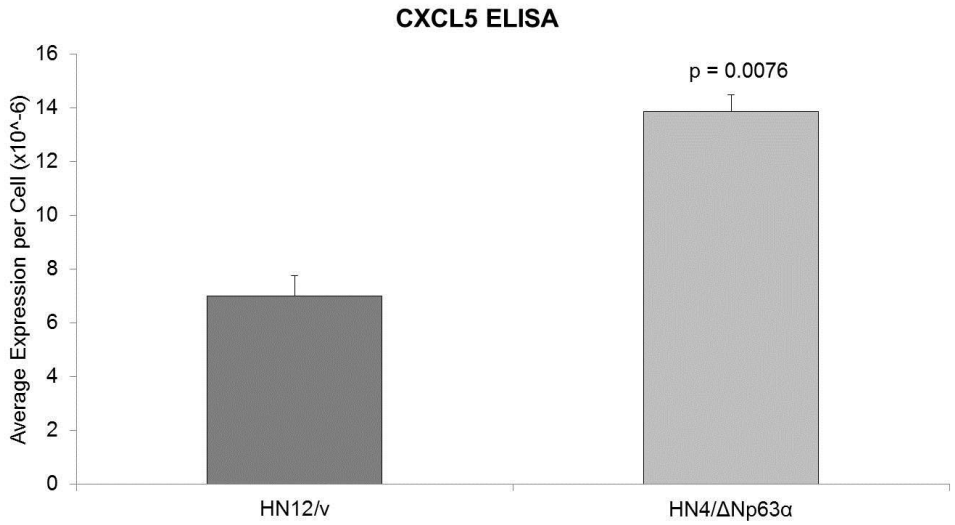

Figure 34. Reduced p63 correlates with elevated CXCL5 protein.
CXCL5 protein expression in two individual G418-selected HN12 clones expressing ΔNp63α as measured by ELISA, normalized to the number of cells per sample. An empty vector HN12 transfectant was used as a control. Data are representative of two independent experiments. (Bar = S.E.M.)

VITA

Brittany Leigh Field was born in Fairfax, Virginia on October 23, 1986. Following graduation from the Mathematics and Science High School at Clover Hill High School in 2004, she attended the University of Virginia for her undergraduate education and graduated in 2008 with a Bachelor of Arts Degree in Biology and a Minor in Chemistry. After earning a Post-Baccalaureate Health Sciences Certificate from Virginia Commonwealth University School of Medicine, she continued to pursue a Master of Science while serving as a teaching assistant for an undergraduate Physiology course. As of Fall 2012, Brittany has matriculated into the Virginia Commonwealth University School of Dentistry.